REMOTELY POWERED UNDERWATER ACOUSTIC SENSOR NETWORKS

A THESIS SUBMITTED TO
THE GRADUATE SCHOOL OF NATURAL AND APPLIED SCIENCES
OF
MIDDLE EAST TECHNICAL UNIVERSITY

ALPER BEREKETLİ

IN PARTIAL FULFILLMENT OF THE REQUIREMENTS
FOR
THE DEGREE OF DOCTOR OF PHILOSOPHY
IN
ELECTRICAL AND ELECTRONICS ENGINEERING

MAY 2013

Approval of the thesis:

REMOTELY POWERED UNDERWATER ACOUSTIC SENSOR NETWORKS

submitted by **ALPER BEREKETLİ** in partial fulfillment of the requirements for the degree of **Doctor of Philosophy in Electrical and Electronics Engineering Department, Middle East Technical University** by,

Prof. Dr. Canan Özgen
Dean, Graduate School of **Natural and Applied Sciences**

Prof. Dr. Gönül Turhan Sayan
Head of Department, **Electrical and Electronics Engineering**

Prof. Dr. Semih Bilgen
Supervisor, **Electrical and Electronics Engineering Dept., METU**

Examining Committee Members:

Assoc. Prof. Dr. Cüneyt F. Bazlamaçcı
Electrical and Electronics Engineering Dept., METU

Prof. Dr. Semih Bilgen
Electrical and Electronics Engineering Dept., METU

Assoc. Prof. Dr. Ece Schmidt
Electrical and Electronics Engineering Dept., METU

Assoc. Prof. Dr. Altan Koçyiğit
Information Systems, METU

Assoc. Prof. Dr. Yusuf Murat Erten
Executive Commitee Member, İnnova A.Ş.

Date: 23.05.2013

I hereby declare that all information in this document has been obtained and presented in accordance with academic rules and ethical conduct. I also declare that, as required by these rules and conduct, I have fully cited and referenced all material and results that are not original to this work.

Name, Last Name: ALPER BEREKETLİ

Signature   :

ABSTRACT

REMOTELY POWERED UNDERWATER ACOUSTIC SENSOR NETWORKS

Bereketli, Alper

Ph.D., Department of Electrical and Electronics Engineering

Supervisor   : Prof. Dr. Semih Bilgen

May 2013, 72 pages

The lifetime of underwater acoustic sensor networks (UASN) is constrained primarily by the power available to the battery-operated sensor nodes. Therefore, power efficiency has become a major design goal for UASN solutions thus far. To eliminate this challenge on the design of UASN, power harvesting is a promising solution, in which Remotely Powered UASN (RPUASN) nodes harvest and store the power available from a powerful external underwater acoustic source. In this study, the novel RPUASN paradigm is introduced and developed. The characteristics of the power harvested from the external acoustic source are analyzed in terms of RPUASN design parameters. The contribution of the ambient noise is investigated in accordance with environmental conditions. Channel characteristics arising from the remote powering configuration are analyzed. Existing MAC, routing, and transport layer protocols proposed for UASN are classified and reviewed. A novel cross-layer protocol, essentially based on CSMA/CA but exploiting the power differential among different RPUASN nodes, is proposed and evaluated comparatively with alternative MAC and routing protocols. It is shown that this new protocol, X-PACCA, achieves acceptable, and under various configurations, superior performance to major competitors. Feasibility is illustrated with realistic examples observing commercial availability of components as a strict constraint. Open research issues are pointed out for reliable communication in RPUASN.

Keywords: Underwater Acoustic Sensor Networks, Power Harvesting, Remotely Powered Underwater Acoustic Sensor Networks (RPUASN), Sink Powered Underwater Acoustic Sensor Networks (SPUASN), Cross Layer Power Adaptive CSMA/CA (X-PACCA)

ÖZ

UZAKTAN BESLEMELİ SUALTI AKUSTİK ALGILAYICI AĞLAR

Bereketli, Alper

Doktora, Elektrik ve Elektronik Mühendisliği Bölümü

Tez Yöneticisi : Prof. Dr. Semih Bilgen

Mayıs 2013, 72 sayfa

Sualtı akustik algılayıcı ağların (UASN) ömrü, temel olarak, pille çalışan algılayıcı düğümlerde mevcut güç ile kısıtlıdır. Bu nedenle, güç verimi, bugüne kadarki UASN çözümleri için büyük bir tasarım hedefi haline gelmiştir. UASN tasarımındaki bu zorluğu ortadan kaldırmak için, uzaktan beslemeli UASN (RPUASN) düğümlerinin güçlü bir dış sualtı akustik kaynaktan gelen gücü hasat edip biriktirdiği *güç hasat etme*, gelecek vadeden bir çözümdür. Bu çalışmada, yeni RPUASN yaklaşımı sunulmakta ve geliştirilmektedir. Dış akustik kaynaktan hasat edilen gücün özellikleri, RPUASN tasarım parametreleri bakımından analiz edilmektedir. Ortam gürültüsünün katkısı, çevresel koşullara uygun olarak incelenmektedir. Uzaktan besleme konfigürasyonundan ortaya çıkan kanal özellikleri analiz edilmektedir. UASN için önerilmiş mevcut MAC, yönlendirme ve taşıma katmanı protokolleri sınıflandırılıp gözden geçirilmektedir. Temel olarak CSMA/CA tabanlı, ancak farklı RPUASN düğümleri arasındaki güç farklarını kullanan yeni bir katmanlar arası protokol önerilmekte ve alternatif MAC ve yönlendirme protokolleri ile karşılaştırmalı olarak değerlendirilmektedir. Bu yeni protokolün, X-PACCA'nın, büyük rakiplerine göre kabul edilebilir ve çeşitli konfigürasyonlar altında daha iyi performans yakaladığı gösterilmektedir. Olurluk, bileşenlerin ticari bulunurluğunu katı bir kısıt olarak gözeten gerçekçi örneklerle gösterilmektedir. RPUASN içinde güvenilir iletişim için açık araştırma konuları ortaya konulmaktadır.

Anahtar Kelimeler: Sualtı Akustik Algılayıcı Ağlar, Güç Hasat Etme, Uzaktan Beslemeli Sualtı Akustik Algılayıcı Ağlar, Alıcı Beslemeli Sualtı Akustik Algılayıcı Ağlar, Katmanlar Arası Güç Uyarlamalı CSMA/CA

To my wonderful wife and best friend, Nuray

ACKNOWLEDGMENTS

Many thanks to FC Bayern München for their world-class virtues, which always inspired me with discipline and persistence. FC Bayern, Stern des Südens, du wirst niemals untergehen, weil wir in guten wie in schlechten Zeiten zueinander stehen. FC Bayern, Deutscher Meister, ja, so heißt er mein Verein. Ja, so war es, und so ist es, und so wird es, immer sein. Mia san mia.

TABLE OF CONTENTS

LIST OF TABLES

TABLES

LIST OF FIGURES

FIGURES

LIST OF ABBREVIATIONS

ACK	Acknowledgment
ARQ	Automatic Repeat Request
AUV	Autonomous Underwater Vehicle
AWGN	Additive White Gaussian Noise
BCH	Bose, Chaudhuri, and Hocquenghem
BER	Bit Error Rate
BFSK	Binary Frequency Shift Keying
BPSK	Binary Phase Shift Keying
CDMA	Code Division Multiple Access
CPU	Central Processing Unit
CSMA	Carrier Sense Multiple Access
CSMA/CA	Carrier Sense Multiple Access with Collision Avoidance
CSP	Control, Sensing, and Processing
CTS	Clear to Send
DI	Directivity Index
EDLC	Electrochemical Double Layer Capacitor
FDMA	Frequency Division Multiple Access
FEC	Forward Error Correction
MAC	Medium Access Control
MACA	Multiple Access with Collision Avoidance
MIMO	Multiple-Input/Multiple-Output
NACK	Negative Acknowledgment
NS	Network Simulator
QPSK	Quadrature Phase Shift Keying
RFEC	Random Forward Error Correction
RPUASN	Remotely Powered Underwater Acoustic Sensor Networks
RTS	Request to Send
RVS	Receiving Voltage Sensitivity
SINR	Signal to Interference plus Noise Ratio
SNR	Signal-to-Noise Ratio
SPUASN	Sink Powered Underwater Acoustic Sensor Networks
TDMA	Time Division Multiple Access

UASN   Underwater Acoustic Sensor Networks

X-PACCA   Cross Layer Power Adaptive CSMA/CA

CHAPTER 1

INTRODUCTION

Underwater communications and data retrieval are required for applications such as marine biology, oceanography, pollution monitoring, sonar, underwater navigation and tracking, weather and climate observation, commercial research, seismic exploration, oil industry, tactical surveillance, and naval operations [1], [2]. Moreover, autonomous underwater vehicles equipped with sensors deliver data to surface stations via underwater communication.

The absorption of electromagnetic energy in the underwater environment is extremely high, about $45\sqrt{f}$ dB per kilometer [9], where f is frequency in Hertz. Therefore, high absorption restricts the use of electromagnetic waves in underwater communication and sonar applications. On the other hand, the absorption of acoustic waves is about three orders of magnitude lower for most of the communication frequency spectrum. Thus, underwater communication networks are based on wireless acoustic communications.

Underwater acoustic sensor networks (UASN) consist of a large number of autonomous sensor nodes densely and randomly deployed to monitor an event area collaboratively. These sensor nodes consist of sensing, processing, and communicating components, and they can only be equipped with small-size batteries, which are limited power sources. Hence, the system lifetime of battery-powered UASN is severely limited by the life span of batteries [1], [4]. So far, most of the research efforts [3], [4], [7] have focused on

- optimization of node placement for better energy efficiency,

- energy-efficient route establishment,

- energy-aware medium access scheduling,

- collision avoidance for reducing energy consumption at retransmissions,

- energy-efficient sleep cycles,

- and proper setting of transmission powers at nodes

to prolong network lifetime. Therefore, the most critical problems for conventional UASN turns out to be energy efficiency and network lifetime constraints, since battery charging in deep water is difficult and expensive [7].

Power harvesting from various sources have been discussed in the literature [8], however, to the best of the author's knowledge, no work has addressed the power requirements of UASN specifically before. In this thesis, the novel concept of *Remotely Powered* UASN (RPUASN) is introduced, where power is supplied to the sensors by an external acoustic source, extending network lifetime indefinitely. Voltage is induced on the harvesting unit of a node, which consists of an array of hydrophones [9]. These harvesting hydrophones operate at the transmission frequency of the external acoustic source, and they do not participate in communication. The power, P_{harv}, harvested at any sensor, can be used for operation or it can be stored in the power unit which consists of a rectifier and a reservoir capacitor. The analysis results reveal that, with a feasible number of commercially available sensor nodes, it is practically possible to achieve 1-coverage and connectivity in RPUASN deployed in a given volume powered by an external acoustic source.

In addition to satisfying the coverage and connectivity requirements in a network, the characteristics of the acoustic channel connecting any two nodes must be studied. To achieve this, it is necessary to investigate the propagation of acoustic waves, which is characterized by three major factors:

- Since the speed of sound (1500 m/s) is low compared to that of the electromagnetic waves, underwater acoustic communication suffers from long and variable propagation delays.

- Attenuation and absorption of acoustic waves increase with signal frequency.

- Underwater acoustic channel yields high bit error rates due to multipath propagation, ambient noise, severely limited bandwidth, and fading.

These factors determine the spatio-temporal characteristics and the capacity of the RPUASN channel, which are dependent on both range and frequency.

RPUASN nodes are autonomous devices with self-configuration capabilities, which can coordinate network operation by exchanging configuration, location, or movement information, and to relay monitored data to an onshore station. For a given node deployment, where harvested power levels are determined, coverage and connectivity are achieved, and channel capacity is estimated, communication protocols are required to gather data successfully throughout the network. It is imperative that sensed event information is reliably transferred over multiple hops by exploiting the shortest path to the data sink. Protocols proposed for conventional UASN have focused mainly on energy efficiency [4]. However, RPUASN are composed of a large number of battery-free nodes, which harvest and store the power supplied by an external acoustic source, indefinitely extending their lifetime. Furthermore, Sink Powered Underwater Acoustic Sensor Networks (SPUASN) constitute a special configuration of RPUASN, where the data sink supplies power to sensors. Hence, removal of the network lifetime constraint, and the specified characteristics of the underwater acoustic channel raise the need for the design of new communication protocols for SPUASN.

In this thesis, we introduce the Cross Layer Power Adaptive CSMA/CA (X-PACCA) protocol for SPUASN. Fully free from lifetime constraints of traditional protocols, X-PACCA integrates MAC, network, and transport layer functionalities. Packet relaying and routing are based on CSMA/CA backoff window size adjustment according to harvested power levels at nodes. End-to-end reliability is enhanced via acknowledgments sent by the sink. Congestion is avoided

via prevention of redundant packet forwarding. Neither global network information nor synchronization is required at nodes. It is shown through simulations that, with appropriate selection of protocol parameters, X-PACCA achieves low end-to-end latency and high throughput, as well as high packet delivery performance.

Hence, the contributions of the thesis can be outlined as follows:

- The novel RPUASN paradigm is proposed, where node operation depends on the power harvested from an external acoustic power source using feasible methods and commercially available components. Numerical examples demonstrate that RPUASN operation is practically realizable with proper choice of design parameters according to channel conditions and sink location. This study has been published in the December 2012 issue of the IEEE Sensors Journal [5].

- Conditions to achieve 1-coverage and connectivity in RPUASN are discussed. The effects of source parameters on coverage are analyzed. The number of nodes required for 1-coverage of a network volume is determined.

- The characteristics of RPUASN channel are discussed. The theoretical limits for the channel capacity in RPUASN are analyzed for variations in ambient noise and interference levels.

- Current literature on the design of communication protocols, specifically medium access control (MAC), routing, and transport layer protocols, is surveyed. Existing protocols are discussed and classified according to their solution approaches.

- The new cross-layer communication protocol, X-PACCA, is proposed for SPUASN. The MAC, routing, and transport layer functions of X-PACCA are explained. The performance of X-PACCA is evaluated and compared against widely known UASN protocols under realistic channel conditions with practical deployment cases. It is shown that appropriate selection of protocol parameters ensure acceptable latency and delivery performance. Our X-PACCA protocol and related performance evaluations are also presented in our paper which is going to appear in the proceedings of MED-HOC-NET 2013 [6].

This dissertation begins with a discussion of the node architecture for the newly proposed RPUASN paradigm. Chapter 2 presents the derivation of the formulation for the harvested power at nodes. The feasibility of RPUASN is discussed in terms of channel characteristics, location, power, and directivity of the source, required power at nodes, and network deployment. Chapter 2 also includes the study on 1-coverage and connectivity for RPUASN in terms of channel and source parameters. Capacity of the RPUASN channel is studied with respect to source and node properties in Chapter 3. Chapter 4 presents a survey of current literature on MAC, routing, and transport layer solutions for conventional UASN. After discussing the advantages and disadvantages of the existing protocols, we propose the novel cross-layer protocol X-PACCA in Chapter 5. Protocol operation is described in detail, and its performance is evaluated through simulations. The simulations compare X-PACCA with several other protocols in terms of end-to-end delay and packet delivery ratio. The dissertation ends with conclusions and a discussion of future work directions in Chapter 6.

CHAPTER 2

REMOTELY POWERED UNDERWATER ACOUSTIC SENSOR NETWORKS

''Nothing is so powerful as an idea whose time has come.''
Victor Hugo

The Remotely Powered Underwater Acoustic Sensor Networks (RPUASN) paradigm is introduced, whereby sensor nodes harvest and store power supplied by an external acoustic source, indefinitely extending their lifetime. Necessary source characteristics are determined. Feasibility is illustrated with realistic examples and open research issues are pointed out. Performance of RPUASN is directly related to the sensing coverage and communication connectivity over the field the sensor nodes are deployed. The required number of RPUASN nodes and the volume which is guaranteed to be covered by the nodes is analyzed in terms of electrical power, range, directivity and transmission frequency of the external acoustic source, and node power requirements.

2.1 Introduction

Lifetime of battery-powered UASN is strictly limited by the life span of batteries [1]. Hence, most of the research efforts have focused on optimization of node placement for better energy efficiency, design of energy-efficient routing and scheduling mechanisms, proper setting of transmission powers, and increasing network lifetime [3], [4], [7]. Therefore, the most critical problem for conventional UASN turns out to be the lifetime constraint, since battery charging in deep water is difficult and expensive [7].

We introduce the concept of RPUASN, in which sensors are powered by an external acoustic source, thereby extending lifetime indefinitely. We then investigate the performance of such networks in terms of sensing coverage and communication connectivity.

Below, we first describe the proposed RPUASN node architecture. Then, we analyze the power harvested to operate such nodes and illustrate the feasibility of remote powering via realistic examples considering practically available components. We then investigate the communication connectivity and sensing coverage provided by such networks under two fundamental scenarios whereby the single remote power source is either situated at the center of a spherical region or on the water surface, powering a conical region underwater. One of the performance parameters we consider is the number of nodes needed to cover a volume powered by a given acoustic source, in terms of the electrical power used by the source as well as the power characteristics

of the sensors. Another performance parameter we investigate is the volume of the deployment region which can be powered by a single source. We conclude the chapter with a brief overview of conclusions.

2.2 Sensor Architecture and Power Budget

While power harvesting from many different sources have been considered in the literature [8], to the best our knowledge, no work has yet explicitly addressed the needs of UASN.

In the proposed network architecture, RPUASN nodes are fed by an external acoustic source. Voltage is induced on the receiver of a passive node, and it is converted to DC. The DC power can either be used to operate the sensor node or kept in a storage capacitor for later use.

2.2.1 Sensor Architecture

A typical RPUASN node hardware is depicted in Fig. 2.1. The node architecture consists of four fundamental units. The control, sensing and processing (CSP) unit performs sensing and data processing. The exchange of information among RPUASN nodes is achieved through the communication transducers. The harvesting unit consists of an array of n hydrophones [9]. The total harvested power is accumulated in the power unit which consists of a DC converter and a reservoir capacitor.
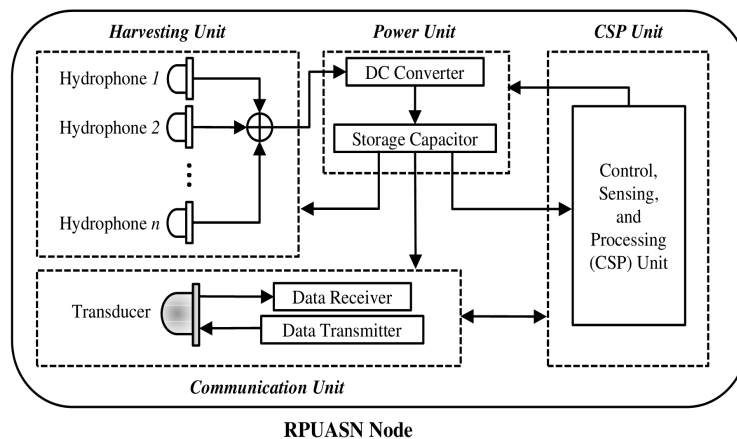
Figure 2.1: Building blocks of an RPUASN node

The electrical behavior of a piezoelectric material is modeled as an induced AC voltage $V_{ind}(t)$ (Fig. 2.2). Power is harvested by connecting the piezoelectric material to the storage capacitor via a rectifier or multiplier circuit. The duty cycle of the harvester circuit may be controlled through a voltage regulator circuit [10]. Since the instantaneous power level stored in the reservoir capacitor may be low, the regulator circuit may also be used to release the stored power in burst mode.

6
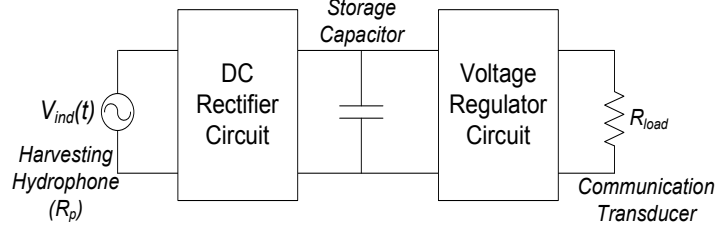
Figure 2.2: Model of the piezoelectric material and the power harvesting circuit

2.2.2 Sensor Power Budget

The source level, SL, in dB re 1 μPa at 1 m, of an underwater acoustic transmitter is given by

$$SL = 170.8 + 10\,log_{10}P_{elec} + 10\,log_{10}\eta + DI \tag{2.1}$$

where DI is the directivity index of the source in dB, and P_{elec} is the electrical input power at the source [11]. The electro-acoustic power conversion efficiency η varies between 0.2 and 0.7 for typical sonar transmitters [9], [11]. Assuming deep water characteristics and neglecting reflection from the air and bottom surfaces throughout the analysis, combining absorption and spherical spreading loss, the total attenuation level (AL) in dB is [9]:

$$AL = 20\,log_{10}R + \alpha\,(f_s)\,R \tag{2.2}$$

where R is the propagation range in m. The absorption coefficient $\alpha(f_s)$ in dB/m increases with frequency and depends on the characteristics of the propagation medium [12]. The difference

$$RL = SL - AL \tag{2.3}$$

gives the received level (RL) in dB at a sensor whose distance to the source is R. Then, the acoustic pressure p on the hydrophone is

$$p = 10^{RL/20} \tag{2.4}$$

which generates voltage at its open circuit terminals. Receiving voltage sensitivity (RVS) of a hydrophone, that accounts for the efficiency of converting incident sound energy to electrical energy, is defined as

$$RVS = 20\,log_{10}M \tag{2.5}$$

in terms of sensitivity M in V/μPa [11]. Using (2.4) and (2.5), the RMS induced voltage is expressed as

$$V_{ind} = pM = \left(10^{RL/20}\right)\left(10^{RVS/20}\right). \tag{2.6}$$

7

According to the well-known maximum power transfer theorem, load power in Fig. 2.2 is maximized if the magnitude of the load impedance (R_{load}) is the same as that of the harvesting hydrophone (R_p). Furthermore, when n hydrophones are connected in series to achieve a higher total induced voltage (nV_{ind}), the total impedance is multiplied by n. Hence, the maximum power available from n hydrophones is

$$P_{available} = \frac{(nV_{ind})^2}{4nR_p} = n\frac{V_{ind}^2}{4R_p} \tag{2.7}$$

where $P_{available}$ is in Watts.

Power losses in recently designed piezoelectric harvesting circuits have become very small compared to the input power, leading to improved efficiencies between 60% and 85% [10]. By substituting Eq. (2.6) into Eq. (2.7) and assuming a realizable harvesting efficiency of 70%, the total power harvested at an RPUASN node with n hydrophones can be obtained as

$$P_{harv} = 0.7n\frac{10^{(RL+RVS)/10}}{4R_p}. \tag{2.8}$$

2.3   Numerical Examples for Feasibility of RPUASN

From the relationships established in the previous section, it can be quantitatively shown that using only commercially available components and devices, underwater sensors can be operated over indefinite lifetimes via remote acoustic powering. In the examples below, the electro-acoustic conversion efficiency of the projector at the source is taken as 50%. Unless otherwise stated, $R_{load} = R_p = 125\ \Omega$ and an RPUASN node includes $n = 5$ hydrophones with sensitivity $RVS = $ -150 dB re V/μPa at the operating frequency of the external acoustic source [11], [13].

2.3.1   Input Electrical Power and Source-to-Node Distance

In this example, source frequency $f_s = 10$ kHz. The source is directional with a DI of 20 dB, which is achievable through a circular piston or disc type projector [9]. As shown in Fig. 2.3, up to a distance of 800 m, the power harvested on each sensor reaches the order of Watts with a source consuming less than 2 kW of electrical power. Below, it will be shown that 100 such nodes, each operating with 200 mW [14] may be powered by a single source to achieve 1-coverage over the full range.

2.3.2   Harvested Power and Source Frequency

The change in the harvested power with frequency is investigated for various R values. In Fig. 2.4, a directional source transmits with $DI = 20$ dB and $P_{elec} = 1$ kW. P_{harv} is almost constant at low frequencies up to $f_s = 20$ kHz. However, for frequencies above 20 kHz, the effect of absorption [12] begins to dominate for R greater than 1 km, reducing the harvested power, as expected from (2.2).
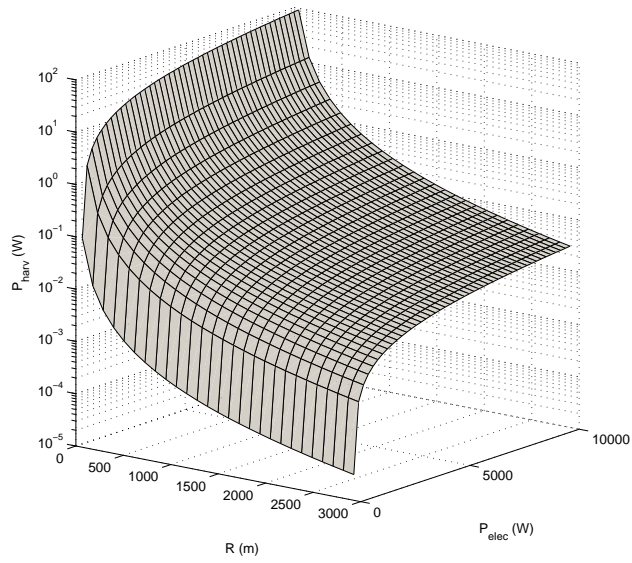
Figure 2.3: Harvested power for electrical input power and distance of the source
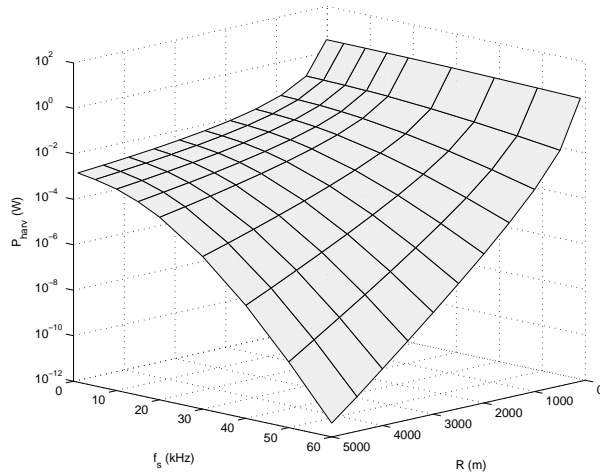
Figure 2.4: Variation of the harvested power with frequency and distance

2.3.3 The Effect of Source Directivity on Harvested Power

To investigate the effect of directivity, P_{harv} is plotted against R for various DI values, as shown in Fig. 2.5. In this case, $P_{elec} = 1$ kW and $f_s = 10$ kHz. In order to provide an RPUASN node with the power level it requires [14], an omnidirectional external acoustic source should be kept closer to the RPUASN node than a directional source.
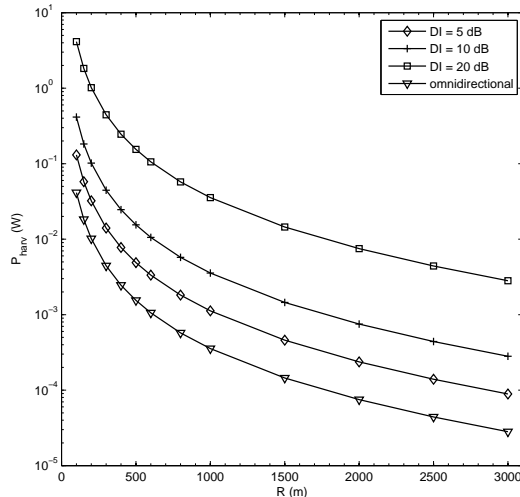
Figure 2.5: Harvested power with distance at various source directivities

2.4 Coverage and Connectivity in RPUASN

In RPUASN, event data must be reliably sensed and communicated to a remote sink via sensor nodes. Therefore, in order to guarantee sensing coverage and communication connectivity, it is important to carefully design the RPUASN deployment according to source and node characteristics.

2.4.1 Required Power and Range

Coverage describes the monitoring quality of a sensor network, and k-coverage implies that every location in the network is monitored by at least k nodes. In order to cover a three dimensional region efficiently while maintaining network connectivity for any given random node deployment, it is vital to estimate the appropriate sensing range, transmission range, and node density. It is assumed that N nodes are deployed randomly and uniformly in a three dimensional region of volume V. Then, each node must have a minimum sensing range (r_s) given by

$$r_s = \left[\frac{-ln\,(1-\delta)\,V}{\frac{4\pi N}{3}} \right]^{1/3} \tag{2.9}$$

where δ is defined as the coverage fraction, which determines the probability that a point in the network is within the sensing range of at least one sensor [15]. It is shown in [16] that ''radius r_s required to achieve a sensing-covered network is greater than the transmission range r_t required to have a connected network''. In agreement with [17], it can be assumed that typically, $r_t \geq r_s$, and *1-coverage implies connectivity* for a given number of nodes in RPUASN. Therefore, the rest of the chapter is based on the minimum r_s to achieve 1-coverage for given N and V. In this discussion, we consider r_s to represent an abstraction of the sensing operation carried

10

out in actual sensors. As such, we take into account actual r_s values of various commercially available devices, but we do not explicitly differentiate between acoustical, electrical, optical, or infrared, etc physical characteristics of individual components. Hence, the operational range of r_s that we consider is sufficiently wide to correspond to a multitude of implementations.

To provide coverage and connectivity in the network, harvested power given by (2.8) should satisfy the minimum power requirement (P_{req}) of an RPUASN node. Using an external acoustic source transmitting with directivity DI and input electrical power P_{elec} at frequency f_s, the maximum range at which an RPUASN node can harvest P_{req} is denoted as R_{max}. For this configuration, the equation for P_{req} can be obtained by inserting the open form for (2.3) into (2.8) as follows:

$$P_{req} = \frac{0.7n}{4R_p} 10^{0.1\left[170.8 + DI + 10\,log_{10}\left(P_{elec}\eta/R_{max}^2\right) - \alpha(f_s)R_{max} + RVS\right]}.$$ (2.10)

Rearranging (2.10) gives the following condition for the maximum range R_{max}:

$$\alpha(f_s)R_{max} + 20\,log_{10}R_{max} = 170.8 + DI + 10\,log_{10}\frac{0.7nP_{elec}\eta}{4R_pP_{req}} + RVS.$$ (2.11)

Two possible deployment scenarios are considered. In the first scenario, RPUASN nodes are dispersed around an omnidirectional acoustic source, as shown in Fig. 2.6. With the valid assumption of spherical spreading in deep water [9], the source is able to supply the power, P_{req}, required by the RPUASN nodes deployed within a spherical region of radius at most R_{max}. In this case, (2.9) can be written as:

$$r_s = \left[\frac{-ln(1-\delta)\frac{4\pi}{3}R_{max}^3}{\frac{4\pi N}{3}}\right]^{1/3} = \left[\frac{-ln(1-\delta)}{N}\right]^{1/3}R_{max}$$ (2.12)

which gives the relation between the radius of the deployment region and sensing range for 1-coverage.

The second deployment scenario is presented in Fig. 2.7. The source is assumed to be a circular piston type projector [11], for which directivity index is related to the vertex angle θ of acoustic transmission by

$$DI = 20\,log_{10}\frac{60\pi}{\theta}.$$ (2.13)

The directed source can supply RPUASN nodes with P_{req} at ranges no greater than R_{max}, and hence, it allows for a deployment volume in the shape of a spherical cone with vertex angle θ and width w, which is the diameter of the spherical cap of the cone. The expression for the minimum sensing range r_s of a node is

$$r_s = \left[\frac{-ln(1-\delta)\frac{2\pi}{3}R_{max}^3\left(1 - cos\frac{\theta}{2}\right)}{\frac{4\pi N}{3}}\right]^{1/3} = \left[\frac{-ln(1-\delta)}{2N}\left(1 - cos\frac{\theta}{2}\right)\right]^{1/3}R_{max}$$ (2.14)

11
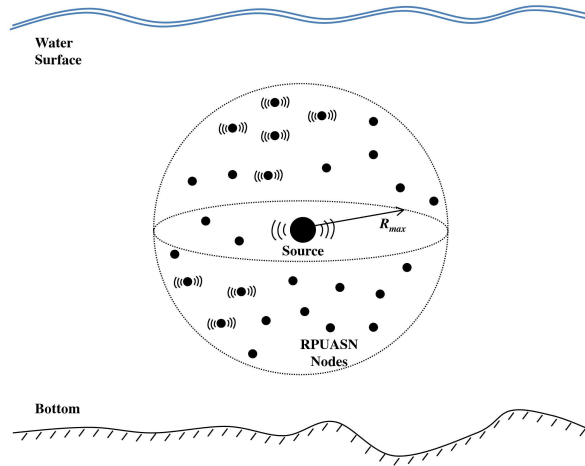
Figure 2.6: RPUASN deployed in a spherical volume
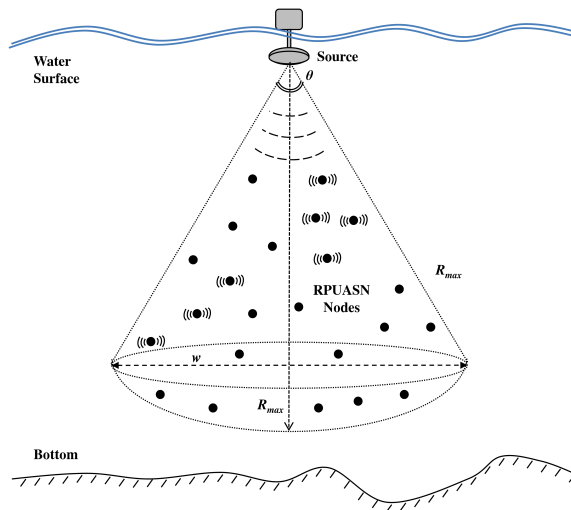
Figure 2.7: RPUASN nodes deployed in a spherical cone for a circular piston source

for guaranteed sensing coverage, and hence communication connectivity.

Consequently, (2.11) and either (2.12) or (2.14) can be used for these two deployment scenarios to determine appropriate design parameters for RPUASN with guaranteed coverage and connectivity, as will be shown in the numerical examples. As stated before, $\eta = 50\%$, R_{load} = R_p = 125 Ω, $n = 5$, and RVS = -150 dB re V/μPa at the source frequency [11], [13]. The required number of nodes is analyzed for a coverage fraction of $\delta = 0.999$ [15]. The power characteristics of sensors are based on commercially available nodes and modems. In particular, P_{req} = 0.2 W [18], [19], P_{req} = 0.5 W [14], [7], and P_{req} = 1 W [20] to account for typical power requirements of RPUASN nodes. The external acoustic source is omnidirectional for spherical deployment (Fig. 2.6), whereas DI = 20 dB for conical deployment, representing a spherical cone with $\theta = 20°$, as shown in Fig. 2.7.
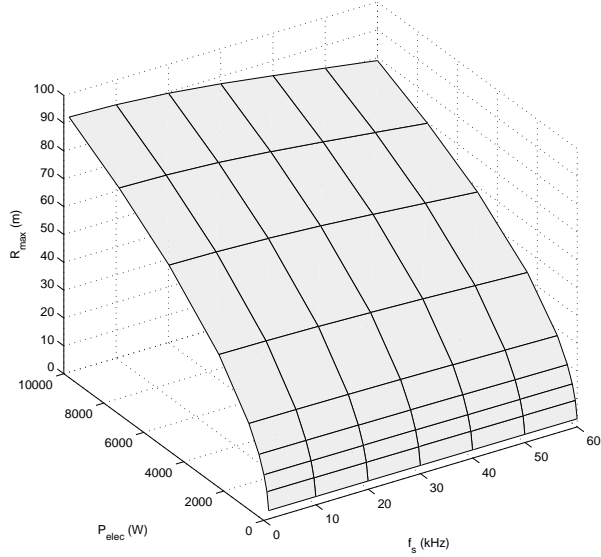
Figure 2.8: Radius of the sphere for source power and frequency
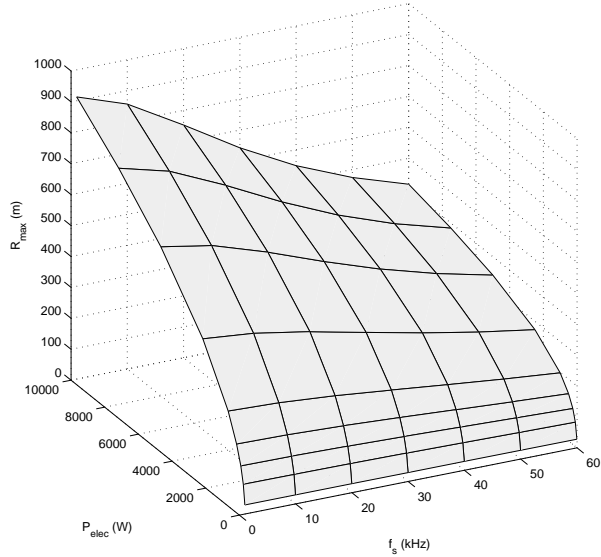
Figure 2.9: Height of the spherical cone at varying source power and frequencies

2.4.2 Volume Powered by The External Acoustic Source

When the source is omnidirectional, the radius of the sphere in which RPUASN nodes can be deployed is given by (2.11). For $P_{req} = 0.5$ W, the source can power nodes at a distance up to $R_{max} = 100$ m for varying P_{elec} at different frequencies, as illustrated in Fig. 2.8. At short ranges, the propagation loss is dominated by spreading but not absorption [12]. Therefore, frequency does not have a major effect for spherical deployment. On the other hand, R_{max} increases from 3 m to 100 m for P_{elec} ranging between 1 W and 10 kW.

R_{max} stands for the height of the spherical cone when the source is a circular piston with DI = 20 dB. The variation of R_{max} with P_{elec} and f_s for this case, again with $P_{req} = 0.5$ W, is

shown in Fig. 2.9. As compared to Fig. 2.8, the effect of absorption is now more visible with frequency, since the source is able to transmit at longer ranges such as 900 m. Combined with directivity, the source transmits at a higher acoustic power intensity, and P_{elec} has a bigger impact on R_{max}. Moreover, for the R_{max} ranges shown in Fig. 2.9, the spherical cone reaches a width of $w = 320$ m. These results show that it is practical to monitor a large volume with sensor nodes powered by a directed acoustic source.
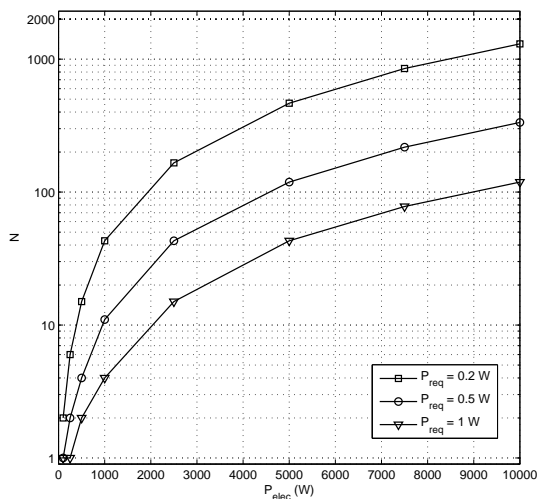
Figure 2.10: Number of nodes in the spherical deployment at varying source power
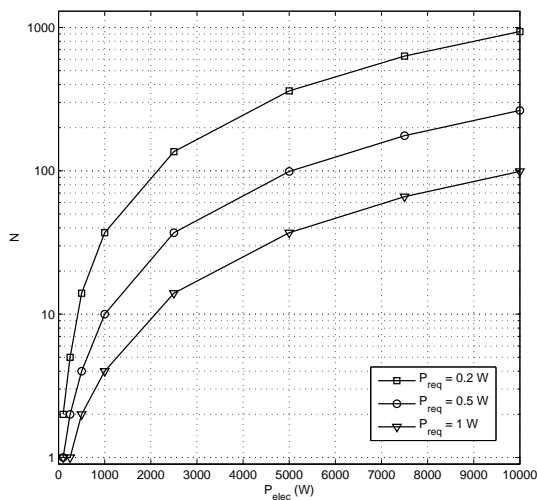
Figure 2.11: Number of nodes in the spherical cone at varying source power

2.4.3 Number of Nodes and Source Power

The number of sensors, N, needed for 1-coverage in spherical and conical deployment scenarios are plotted against source power in Fig. 2.10 and Fig. 2.11, with r_s set to 25 m and 50 m,

14

respectively [15]. When P_{elec} is increased, the source supplies power to a longer range. As a result, the volume of the sphere in which nodes are deployed increases. Increasing the network size necessitates coverage and connectivity over a larger region, and this implies a higher number of nodes, since the range of each node is limited by r_s. Hence, N stands for the minimum number of sensors that may be powered by a source consuming the electrical power, P_{elec}, to achieve 1-coverage within its full range.

Figures 2.10 and 2.11 show that increasing P_{req} requires a stronger source to supply power to a given number of sensors if the source-to-sensor distances remain the same. A stronger source can supply an increased number of nodes with a certain P_{req} to achieve 1-coverage within its full range.

2.4.4 Number of Nodes and Sensing Range

An event field can be covered by a smaller number of RPUASN nodes if the sensing range of nodes is increased. In Fig. 2.12 and Fig. 2.13, the selected r_s values are based on commercially available components and P_{req} is assumed to be 0.5 W [14]. Using a higher source power enables a higher number of nodes with a given sensing range, r_s, providing 1-coverage within a larger volume.
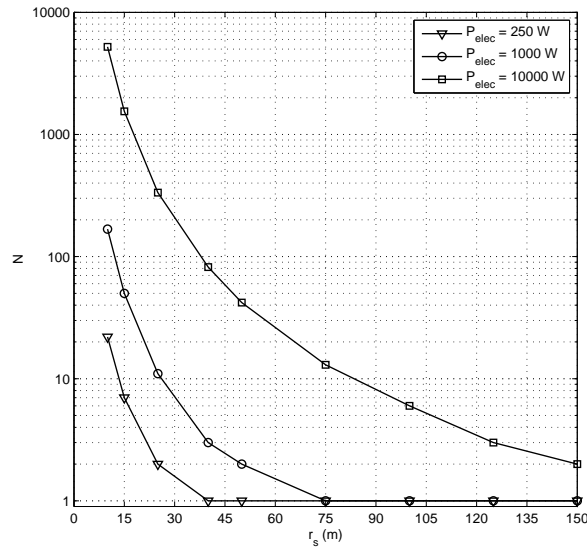
Figure 2.12: Variation of N with sensing range for the spherical deployment

The results for the spherical cone scenario are plotted in Fig. 2.13. Transmitting with $DI = 20$ dB, the source reaches a longer R_{max} and allows for a larger deployment region, enabling a higher number of nodes achieving 1-coverage over that volume in comparison to Fig. 2.12.

These examples show that it is practically possible to achieve 1-coverage and connectivity in a given volume powered by a given acoustic source with a feasible number of commercially available ([13]-[15], [18]-[20]) sensor nodes.

15
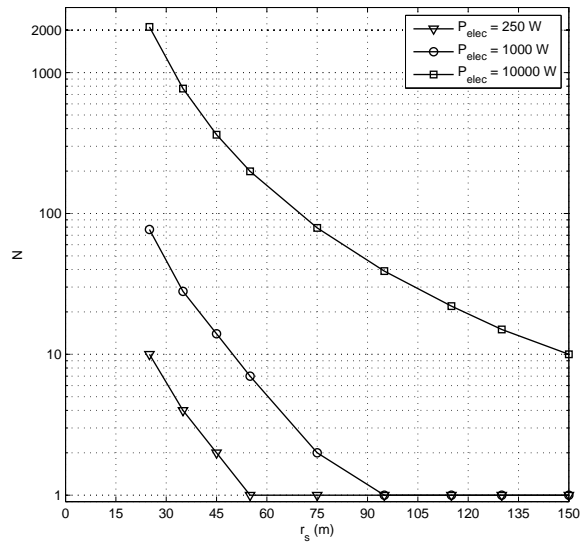
Figure 2.13: Variation of N with sensing range for the spherical cone

2.5   Conclusion

A novel paradigm whereby underwater sensors are powered by a remote acoustic source is presented and its feasibility in terms of source power and source-to-node distance is investigated. Numerical examples demonstrate that sensor operation is practically realizable with proper choice of design parameters. In the subsequent chapters, appropriate protocol stacks are studied according to the channel model and communication requirements, considering the newly proposed concept of remotely supplied operating power.

CHAPTER 3

CHANNEL CAPACITY IN RPUASN

"A clever person solves a problem. A wise person avoids it."
Albert Einstein

The RPUASN paradigm is studied in terms of the channel characteristics achieved under various realistic conditions. Placing the power source on the water surface, leading to a conical region of sensor deployment is considered. Variation of channel capacity with operating frequency and interference levels is determined. Rather than specific MAC protocols that guarantee interference-free operation, a theoretical parametric constraint of silence of neighboring sensor nodes is imposed on the network, thereby allowing investigation of upper and lower bounds of communication capacity. Effect of the sensing range of nodes on channel capacity, as well as SINR and BER characteristics, are also studied. It is shown that practical configurations that use commercially available components lead to feasible communication capacities.

3.1 Introduction

In Chapter 2, it is quantitatively shown that using commercially available components, *underwater sensor networks can be operated over indefinite lifetimes via remote acoustic powering.* In that study, the electro-acoustic conversion efficiency of the source is taken as $\eta = 50\%$. An RPUASN node is assumed to include $n = 5$ hydrophones with impedance R_p = 125 Ω and receiving sensitivity RVS = -150 dB re V/μPa at the operating frequency of the external acoustic source [11], [13]. With the external acoustic source transmitting at f_s = 10 kHz with a directivity of DI = 20 dB, the variation of P_{harv} at an RPUASN node for source-to-node distance R and source power P_{elec} is shown in Fig. 2.3. To guarantee proper network operation, P_{harv} must satisfy the power requirement (P_{req}) at each node. Up to 800 m, the power harvested on an RPUASN node is on the order of Watts, with the source powered by less than 2 kW. It is also shown that 100 nodes, each operating with around 200 mW [14] may be powered by a single external acoustic source to achieve 1-coverage over the full range of the source.

In this chapter, we investigate the channel capacity achieved in RPUASN. Our objective is to acquire an insight into the theoretical limits of RPUASN channel capacity. Hence, for the sake of simplicity, we neglect the effect of multipath fading on acoustic signals in our analysis.

Below, we first describe the network model for analyzing the channel capacity of RPUASN. We briefly discuss the underwater channel characteristics as they are the key factors in determining

the received and harvested power levels at nodes. Then, we define and investigate the RPUASN channel capacity under the fundamental deployment scenario where the acoustic source is situated on the water surface, powering a conical region underwater. The parameters in the capacity analysis are communication frequency, sensing range, number of interfering nodes, and wind speed.

3.2   Network Model

Although the spherical deployment topology is also shown to be feasible in Chapter 2, in this chapter we consider only conical deployment, which is shown in Fig. 2.7, as this is the most practical in terms of versatility of power source location at the water surface. The maximum distance of any sensor from the source for harvesting sufficient power, i.e., at least P_{req}, is denoted by R_{max}.

Coverage and connectivity issues of 3D networks, in general, are investigated in [21], with the goal of finding a node placement strategy that guarantees 100% coverage of a 3D space using the minimum number of nodes with a given sensing range r_s. The results indicate that the number of nodes to achieve coverage with hexagonal prism placement strategy is almost half of the number required by cubic grid deployment strategy. Therefore, we adopted the use of hexagonal lattice to deploy RPUASN nodes for our channel capacity analysis. Similar to [21], the coordinates of nodes are determined with respect to the center of the lattice and the sensing ranges of nodes.

3.3   RPUASN Channel Characteristics

In an underwater acoustic channel, attenuation over a distance d for a signal of frequency f is given by

$$A(d, f) = d^\kappa a(f)^d \tag{3.1}$$

where $a(f)$ is the absorption coefficient and κ is the spreading factor. The absorption coefficient in dB/km is given in terms of frequency f (in kHz) by Thorp's formula [22]

$$10 log_{10} a(f) = \frac{0.11 f^2}{1 + f^2} + \frac{44 f^2}{4100 + f^2} + \frac{2.75 f^2}{10^4} + 0.003. \tag{3.2}$$

as also stated in Eq. 2.2 before.

The other factor which can be used in the characterization of RPUASN channel is isotropic ambient noise. Underwater ambient noise can be described by Gaussian statistics [24], and, for the sake of simplicity, our analysis is based on this valid additive white Gaussian noise (AWGN) assumption. Underwater noise may arise from turbulence $N_t(f)$, shipping activity $N_s(f)$, surface agitation $N_w(f)$, and thermal noise $N_{th}(f)$. The following expressions give the spectral densities of these different noise components in dB re μPa^2 per Hz as a function of frequency f in kHz [22]

$$
\begin{aligned}
&10 log_{10} N_t(f) = 17 - 30 log_{10} f \\
&10 log_{10} N_s(f) = 40 + 20(s - 0.5) + 26 log_{10} f - 60 log_{10}(f + 0.03) \\
&10 log_{10} N_w(f) = 50 + 7.5 \sqrt{w} + 20 log_{10} f - 40 log_{10}(f + 0.4) \\
&10 log_{10} N_{th}(f) = -15 + 20 log_{10} f
\end{aligned}
\tag{3.3}
$$

where each component impacts the spectral density at different frequencies [23]. Turbulence is the main noise source between 1 Hz and 10 Hz. Over the next decade, shipping activity is the major cause of ambient noise. On the other hand, noise between 100 Hz and 100 kHz is produced by surface agitation due to wind. Finally, at 100 kHz and beyond frequencies, noise is dominated by thermal noise. The overall noise power spectral density in μPa^2 per Hz, which is depicted in Fig. 3.1, is given by

$$N_d(f) = N_t(f) + N_s(f) + N_w(f) + N_{th}(f). \tag{3.4}$$
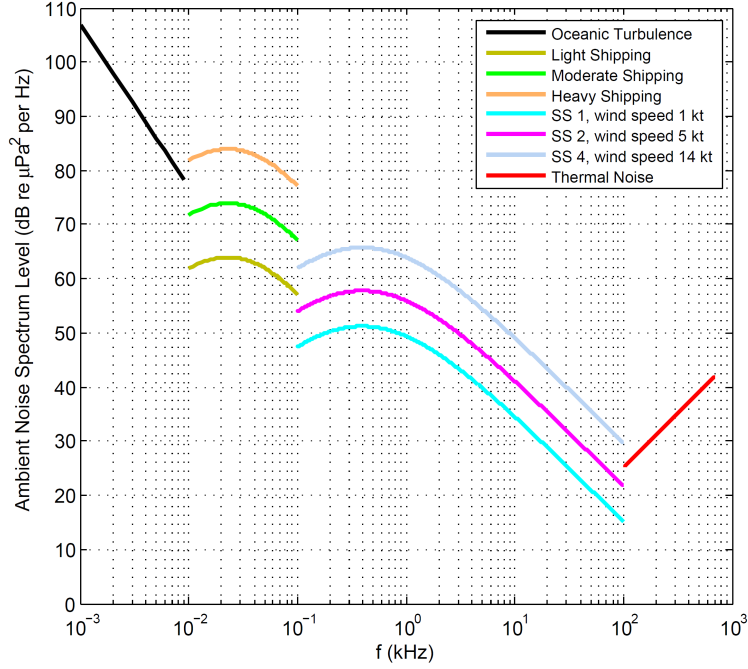
Figure 3.1: The overall noise power spectral density in the underwater environment

Acoustic intensity (ϕ) is related to pressure (p) through the acoustic impedance of the underwater medium as follows

$$\phi = p^2/Z \tag{3.5}$$

where $Z = 1.5$ Mrayl for sea water [9]. Hence, for $p = 1$ μPa, we obtain $\phi = 6.7{\times}10^{-19}$ W/m$^2\mu\text{Pa}^2$. For a noise spectral density of $N_{dB}(f) = 10log_{10}N_d(f)$ in dB re μPa^2 per Hz, the equation

$$N(f) = \left(6.7{\times}10^{-19}\right)10^{N_{dB}(f)/10} \tag{3.6}$$

gives the resulting noise power spectral density in W/Hz for a surface of 1 m^2.

We consider a network where each node has a harvesting unit and a communication unit, as described in Chapter 2, deployed according to the source location such that each node harvests at least P_{req} and all nodes transmit with $P_t = 0.2P_{harv}$, which is a feasible power budget usage assumption [25].

In order to illustrate the effect of interference on communication quality and channel capacity, we concentrate on a single transmission at frequency f from node i to the receiver r, which are d_i apart from each other. With the attenuation over d_i found using (3.1), the received signal power can be written as

$$P_r(f) = P_{t,i}(f)/A(d_i, f) = P_{t,i}(f)/d_i^\kappa a(f)^{d_i}. \tag{3.7}$$

For the interference, we set a medium access control (MAC) protocol constraint similar to the one in [24]. In our constraint, a node j is not aware of the transmission from i to r if its distance to r is beyond the limit determined by an interference parameter m. That is, node j may create interference if its distance to the receiver (d_j) is greater than or equal to mr_s. Otherwise, we assume that node j is aware of the communicating pair, and it remains silent. As a result, the total interference power at the receiver is

$$I_r(f, m) = \sum_{\substack{j \neq i \\ d_j \geq mr_s}} P_{t,j}(f)/A(d_j, f) \tag{3.8}$$

for a given m determined by the capability of the medium access protocol. Consequently, using (3.6)-(3.8) for a communication frequency f and bandwidth B, the signal to interference plus noise ratio (SINR) at the receiving node r can be calculated as

$$SINR(f) = \frac{P_r(f)}{I_r(f, m) + BN(f)}. \tag{3.9}$$

Using the result in (3.9), channel capacity can be found by

$$C(f) = B \ log_2 \left(1 + SINR(f) \right) \tag{3.10}$$

where $C(f)$ is the Shannon capacity of the channel in bits per second.

For this configuration, the ratio of energy per bit (E_b) to noise power spectral density (N_0) can be calculated as [26]

$$\frac{E_b}{N_0} = \frac{B}{C(f)} SINR(f) \tag{3.11}$$

for the AWGN channel. Using (3.11), the bit error rate (BER) can be determined as

$$BER = Q\left(\sqrt{2E_b/N_0}\right) \tag{3.12}$$

assuming BPSK or QPSK modulation. Similarly, for BFSK, the error rate is

$$BER = Q\left(\sqrt{E_b/N_0}\right) \tag{3.13}$$

using the Gaussian Q-function [27].

3.4   Numerical Analysis

RPUASN channel capacity is investigated for varying communication frequency f, sensing range r_s, interference parameter m, and wind speed w. The network is a hexagonal lattice of 125 nodes with the power requirement of $P_{req} = 0.5$ W. The external acoustic source transmits with $P_{elec} = 10$ kW at $f_s = 10$ kHz. Assuming a practical value [24] of $\kappa = 1.5$ for the spreading coefficient, R_{max} is found to be 5146 m for conical deployment, using the relations derived in Chapter 2. The directed source, i.e., having $DI = 20$ dB, is at a distance of 3500 m from the center of the lattice. The receiving node r is located at the center of the lattice, with the transmitting node i being its closest neighbor. Unless otherwise stated, communication bandwidth is taken as $B = 3$ kHz, and the shipping activity parameter for ambient noise is $s = 0.5$.

3.4.1 Communication Frequency

The variation of $C(f)$ with f at different levels of interference is shown in Fig. 3.2. Wind speed is taken as $w = 4$ m/s, i.e., sea state 2 with a gentle breeze. For a given m, absorption increases with frequency, diminishing the effect of interfering nodes and raising SINR. Beyond $f = 100$ kHz, ambient noise is dominated by thermal noise and not wind speed. The level of ambient noise at such high frequencies is much lower, and in a certain frequency interval, the decay of the noise spectral density can be assumed to be linear in the logarithmic scale, with an approximate decay rate of 18 dB/decade [26]. Therefore, the contribution of ambient noise in SINR becomes almost negligible for a specific m, and there is not a major change in channel capacity above 100 kHz.
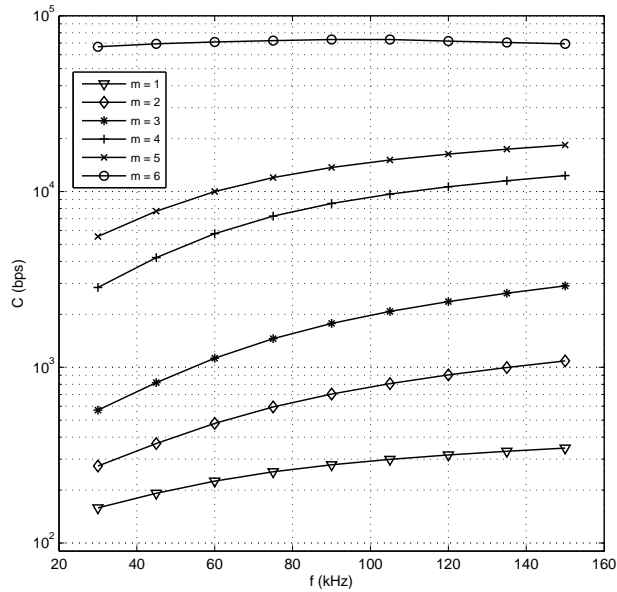
Figure 3.2: Variation of channel capacity with frequency

The worst case channel capacity is above 100 bps. Increasing m in (3.8) means reducing the number of interfering nodes, thereby raising SINR and channel capacity at a given frequency. Using $r_s = 100$ m for $m = 6$ leads to zero interference. Hence, SINR for $m = 6$ is equal to the signal to noise ratio (SNR) at the receiver (with all nodes kept silent). The results are promising, since provided that interference is sufficiently suppressed, corresponding to, say, $m = 6$, possibly with a properly designed MAC protocol, data rates of up to 70 kbps are theoretically realizable. With current commercially available hardware, operation at 38.4 kbps must be practically possible [20].

3.4.2 Sensing Range of Nodes

In order to guarantee 1-coverage within a given volume using the minimum number of nodes, increasing r_s means a smaller number of nodes satisfy the coverage requirement. For a wind speed of $w = 4$ m/s, the effect of sensing range on capacity at $f = 30$ kHz is shown in Fig. 3.3. At a given w, changing the range from 10 m to 100 m does not yield a major effect on the

channel capacity. When there is no interference, i.e., $m = 6$, the capacity is determined by SNR, and channel capacities of 70 kbps are achieved. For a given interference parameter m, the product mr_s is increased with a higher sensing range. Therefore, more nodes can be kept silent, increasing the capacity slightly.
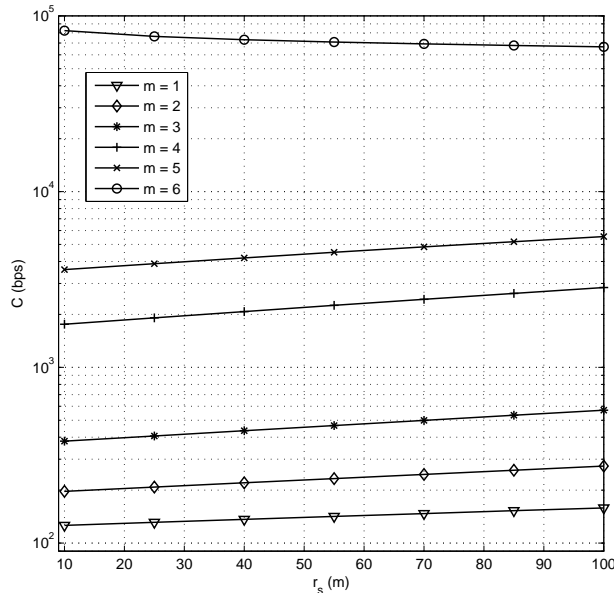
Figure 3.3: Channel capacity vs. sensing range at different levels of interference

The variation of channel capacity with sensor range, when all interference is suppressed, i.e. $m = 6$, is given in Fig. 3.4. Even with a high wind speed of 24 m/s, RPUASN nodes are able to obtain a channel capacity of 50 kbps, provided that there is no interference and the communication quality is determined by SNR. As long as interference-free operation is maintained, the theoretical capacity limit becomes independent of node deployment.

3.4.3 Frequency and Sensing Range

The dependence of RPUASN channel capacity on communication frequency and sensing range is shown in Fig. 3.5. In this figure, $w = 4$ m/s and all nodes other than the transmitter are assumed to be silent; hence, we present the maximum achievable data rates in RPUASN with 125 nodes. Channel capacity rises for frequencies up to 100 kHz and for higher frequencies, begins to decay due to the combined effect of the attenuation and noise, which is in compliance with related studies [26]. Regardless of deployment topology, the worst case theoretical capacity is above 65 kbps.

3.4.4 SINR and BER

For the practical case of conical deployment, the change of SINR with frequency is shown in Fig. 3.6. Wind speed is $w = 4$ m/s and node range is $r_s = 100$ m. When there is too much interference in the network ($m = 1$), the achieved SINR fails to exceed -10 dB for the entire frequency band, from 30 kHz to 150 kHz. To obtain a positive SINR, the interference
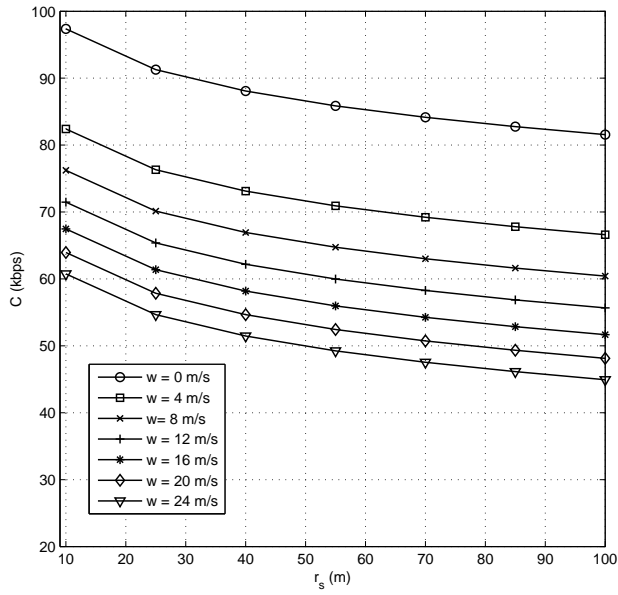
Figure 3.4: Capacity vs. node range at varying wind speed
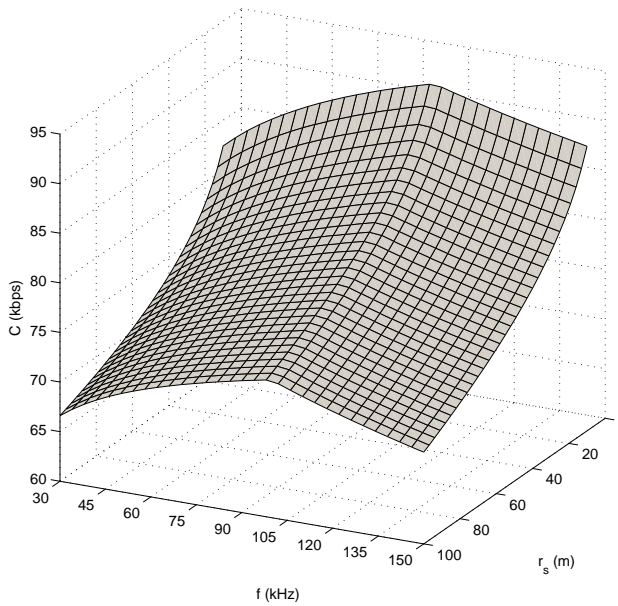
Figure 3.5: RPUASN channel capacity for frequency and sensing range

parameter m should be at least 4, that is to say, nodes at a distance up to $4r_s$ from the receiver should be kept silent. Absorption increases with frequency [22], but ambient noise has less effect on communication at higher frequencies, as expressed in (3.3). Therefore, due to the combined effect of absorption and noise, SINR increases slightly with frequency until $m = 6$. For $m = 6$, there is no interference, and the channel quality is solely determined by SNR according to the joint behavior of absorption and noise [26].
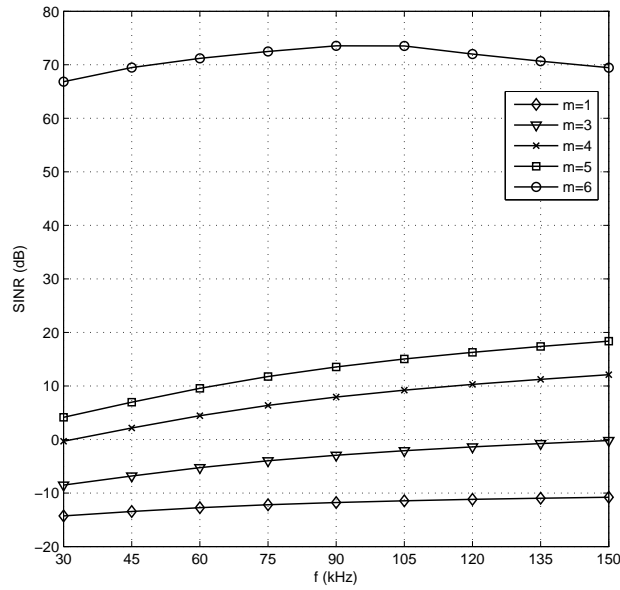
Figure 3.6: The change of SINR with frequency

The variation of BER against frequency is presented in Fig. 3.7. For the RPUASN channel, error rate values are shown for BPSK (or, equivalently, QPSK) and BFSK modulation schemes for underwater acoustic communication [26]. As expected from Fig. 3.6, a lower BER is achieved for higher frequencies and at larger m. With BPSK, an interference parameter of $m = 4$ is satisfactory to obtain an RPUASN channel BER less than 0.01. For BFSK, m should be at least 5 to achieve the same BER. However, interference-free network operation will yield much smaller BER values, as realized from the rise in SINR with $m = 6$ in Fig. 3.6.
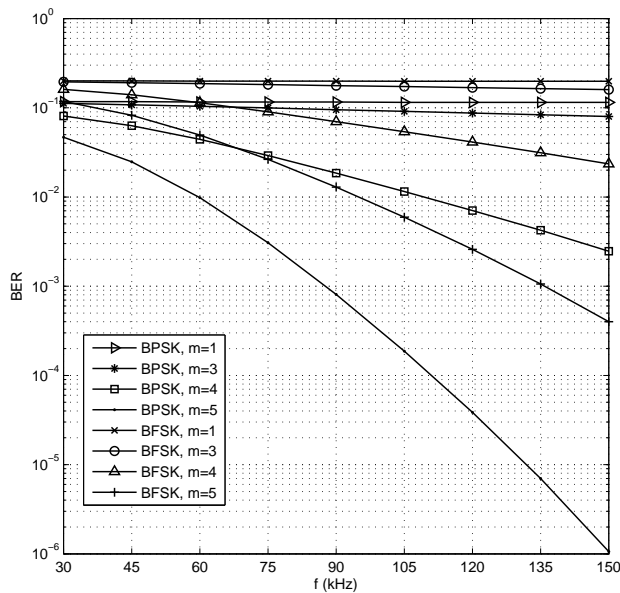
Figure 3.7: BER and frequency for conical deployment

3.5 Conclusion

The quality of an RPUASN channel is investigated in terms of channel capacity, SINR, and BER for different digital modulation types. As shown in Fig. 3.5, the channel capacity is able to meet the requirements of underwater acoustic communication. However, as seen in Fig. 3.6 and Fig. 3.7, a certain number of nodes should be kept silent for higher SINR and lower BER, showing that the key step in providing a higher channel quality is imposing the necessary medium access protocol constraints. Therefore, in the succeeding chapters, we first study the characteristics of the protocols proposed for UASN, and then we propose an appropriate protocol structure for RPUASN.

CHAPTER 4

MAC, ROUTING, AND TRANSPORT LAYER PROTOCOLS FOR UASN

''If you cause your ship to stop, and place the head of a long tube in the water, and place the other extremity to your ear, you will hear ships at a great distance from you.''

Leonardo da Vinci (1490)

In this chapter, current literature on MAC, routing, and transport layer protocols for UASN is discussed. Protocols are briefly explained and summarized according to their solution approaches.

4.1   MAC Protocols

A number of solutions have been proposed for the medium access problem in conventional UASN [28]. Deterministic MAC schemes such as Time Division Multiple Access (TDMA), Frequency Division Multiple Access (FDMA), or Code Division Multiple Access (CDMA) cannot be directly adopted in the underwater environment due to problems such as narrow channel bandwidth, vulnerability to fading and multipath, dependence on network-wide clock synchronization, handling long propagation delays, optimizing energy consumption, difficulty of power control at each node to avoid the near-far problem, and scalability with number of nodes [3]. Therefore, majority of the solution efforts have led to random access protocols mostly based on carrier sense multiple access with collision avoidance (CSMA/CA). According to their medium access strategies, MAC solutions proposed for UASN can be classified as contention-based (using RTS/CTS exchange), CSMA-based, reservation-based, or ALOHA-based protocols, as discussed in Table 4.1. The main performance criteria in these protocols are energy efficiency and network lifetime, since conventional UASN nodes run on limited-capacity batteries.

Table4.1: MAC Protocols for UASN

Protocol	Classification	Remarks
APCAP [29]	• RTS/CTS exchange • Time slotting	• Multiple time slots can be reserved by a single node. • Nodes require an absolute time reference. • A scheduled transmission cannot be canceled even if another one is detected.

Table 4.1 (cont'd)

Protocol	Classification	Remarks
DACAP [30]	• RTS/CTS handshaking	• Nodes' tolerance to interference is utilized to minimize handshaking delay. • Nodes are assumed to transmit with the same power.
Ordered CSMA [31]	• CSMA-based • Round robin scheduling	• Avoids control packet handshaking. • Centralized coordination requires relative locations of all nodes. • TDMA with reduced guard times.
SF-MAC [32]	• RTS/CTS handshaking	• Transmission order is determined at the receiving side, after the receiver waits for RTS from all contenders. • Fairness is achieved at the expense of channel utilization.
Slotted FAMA [33]	• FAMA-based • Carrier sensing • Time slotting	• Degrades energy consumption by removing the need for control packets. • Relies on global time synchronization. • Nodes are allowed to transmit only at the beginning of a time slot.
R-MAC [34]	• Reservation-based	• Based on the estimation of propagation delays; requires neighbor discovery. • No centralized scheduling or synchronization.
T-Lohi [35]	• Reservation-based	• Single-hop MAC assumption. • Based on estimating the number of contenders. • Random backoff promotes fairness.
UWAN-MAC [36]	• Reservation-based • TDMA-like	• Energy is the main performance metric. • Appropriate only for stationary nodes. • Requires synchronization through periodic message exchange.
RIPT [37]	• Reservation at the receiver with packet trains	• Generates packet exchange overhead. • For a dynamic topology, it is not practical to schedule transmissions at each node.
PCAP [38]	• RTS/CTS handshaking	• Receiver waits for an additional duration before replying an RTS with a CTS. • Accurate timing is required among nodes. • Protocol operation depends on the estimation of propagation delay between any two nodes.

Table 4.1 (cont'd)

Protocol	Classification	Remarks
Aloha-CA, Aloha-AN [39]	• Aloha-based	• Protocols use propagation delays between every node pair in the network. • Mobility of nodes and dynamic topologies generate errors in delay calculations and position estimations. • Nodes extract sender/receiver information from every packet they overhear. • Single-hop MAC.
MACA-MN [40]	• RTS/CTS handshaking • MACA-based	• A packet train is formed for multiple neighbors to achieve high throughput. • Sender has to know the propagation delay from itself to all intended receivers. • CTS packets collide when the receivers are at the same distance from the sender.
MACA-U [41]	• RTS/CTS handshaking • MACA-based	• State transitions of MACA are defined according to propagation delays. • Packets are assigned different priorities to avoid starvation in case of simultaneous transmission attempts.
UW-MAC [42]	• CDMA-based • Aloha-like	• The optimal transmit power and code length are determined at the transmitter. • The received signal and the direct-sequence CDMA code must be synchronized. • Near-far problem encountered in CDMA must be minimized by optimizing the transmission power.
ST-MAC [43]	• TDMA-based	• Focused on spatio-temporal uncertainty. • Network information is collected at the sink, and vertex coloring is used to schedule transmissions.
BiC-MAC [44]	• Packet bursting • Handshaking	• Sender triggers the handshake, and any receiver can initiate bidirectional packet burst. • Every node has to know the propagation delay from each of its neighbors to itself, which is estimated and disseminated during the network initialization phase.
UW-MAC [45]	• CDMA-based • Clustering • TDMA scheduling	• Nodes use neighborhood and battery lifetime information to form clusters. • CDMA within a cluster. • Cluster heads communicate with the sink with a TDMA schedule. • Near-far problem in CDMA and scheduling overhead of TDMA must be investigated.

Table 4.1 (cont'd)

Protocol	Classification	Remarks
DOTS [46]	• CSMA-based • TDMA scheduling	• Nodes overhear messages to learn the transmission schedules and propagation delay of their neighbors. • Clock synchronization is assumed. • Provides fairness and mobility support via CSMA, however, no collision is assumed for control packets.
Q-CSMA [47]	• CSMA-based • Time slotting	• Each time slot is divided into control and data slots. Collisions are allowed in control slots, in which transmissions are scheduled. • A discrete-time version of CSMA, where multiple links can update states in a time slot. • Scalability of the protocol with graph size and multi-hop traffic must be investigated in terms of network delay performance.
ROPA [48]	• Packet bursting	• Avoids the need for separate handshakes for each communication pair. • Prevents hidden nodes by using information extracted from control packets. • Appropriate for static networks, where nodes have little or no mobility.
EHM [49]	• RTS/CTS handshaking	• The receiver captures RTS from potential senders and replies with a CTS broadcast. • Each node needs to know the propagation delays to its neighbors. • Nodes have to broadcast their routing tables periodically.
CT-MAC [50]	• MIMO uplink communication with the sink • Prioritizing	• Nodes exchange information locally and gather global state via relays. • Single-hop MAC to transmit to the sink. • Global time synchronization is assumed.
STUMP [51]	• TDMA-based	• Uses node position diversity via estimation of propagation delays to schedule transmissions. • With the help of synchronization, nodes share delay estimates and time slot requirements with their two-hop neighbors. • Nodes are assumed to be stationary for the accuracy of estimation.

Table 4.1 (cont'd)

Protocol	Classification	Remarks
ISTLS [52]	• TDMA-based • Time slotting	• A slotted conflict graph is constructed. It is based on network topology, propagation delay, and link transmission delay information. • Network-wide clock synchronization is required. • Nodes are assumed to be static.

CSMA and its variations [31], [33], [40], [41], [46], [47] have been preferred in order to prevent collisions between two or more stations transmitting at the same time, which occurs frequently in ALOHA-based protocols [39], [45].

The handshaking protocol in [29] requires synchronization of all nodes. A node is allowed to reserve multiple time slots, and the scheduled transmission cannot be canceled even if another communicating neighbor is detected. In [30], an RTS/CTS handshaking solution that does not need clock synchronization is proposed. However, RTS/CTS handshaking brings extra delay to MAC operation. The protocol assumes that all nodes use the same transmission power, which is not valid for SPUASN. To solve any uncertainty, coordination of medium access is carried out by a centralized controller in [31]; however, deciding on a network-wide collision-free transmission order requires knowledge of relative locations of all nodes. It is also proposed to choose a transmission order at the receiver side [32]. The receiver has to wait until it receives an RTS from all possible contenders, and this decreases channel utilization seriously. [33] combines carrier sensing with a packet exchange between sender and receiver before transmission. Nodes rely on global time synchronization, and a node is allowed to transmit only at the beginning of a time slot.

Reservation-based MAC is another design alternative [34]-[37]. Nodes estimate propagation delays for scheduling transmissions in [34]. However, this estimation is applicable when nodes are static and no new node joins the network. [35] is a MAC solution for single-hop networks, where each node counts the number of contenders for the channel. [36] is a TDMA implementation requiring synchronization of transmission schedules through periodic message exchange. Similarly, in [37], [44], and [48], receivers periodically start packet transfers, generating continuous overhead in the network. Furthermore, for a dynamic topology under channel fluctuations, it is not very practical to determine when to initiate transmission at each node.

UWAN-MAC [36] has the objective of coordinating multiple access by limiting contentions. Neighboring nodes broadcast their sleep schedules to each other, so that each node can infer the instants to wake up. However, protocol performance is degraded by the limitations resulting from long acoustic propagation delays, which constrain throughput. Another highly-cited MAC solution, Slotted FAMA [33] makes use of both handshaking and carrier sensing to save energy by collision avoidance. All nodes in the network are synchronized, and RTS/CTS handshakes are initiated only at the beginning of a time slot. This method is effective in reducing collisions. On the other hand, it limits throughput because of the long guard durations between consecutive slots.

4.2 Routing Protocols

An underwater acoustic sensor network consists of a large number of nodes deployed at different depths, performing multi-hop communication realized by appropriate routing schemes. Conventional underwater routing schemes are based on the availability of network resources and the efficient use of limited battery power at nodes [53]. Routing protocols for UASN are summarized in Table 4.2.

Table4.2: Routing Protocols for UASN

Protocol	Classification	Remarks
FBR [54]	• Hop-by-hop • Demand-based • Geographical	• Nodes try to find relays within a conical volume towards the sink by transmitting RTS multicast packets at increasing power levels. • A data source must be aware of its own location and the fixed location of the sink. • Forwarding volume and transmission power affect route setup delay and RTS overhead.
REBAR [55]	• Hop-by-hop • Demand-based • Hierarchical • Geographical	• Network is divided into tiers according to energy depletion and communication ranges of nodes. • Multi-path redundancy is exploited to increase packet delivery ratio. • A source knows its location and that of the sink. • Building the protocol according to changes in node positions yields to packet delivery failures when nodes are static.
VBF [56]	• End-to-end • Demand-based • Geographical	• Operation depends on the locations of the source, forwarding nodes, and the sink. • Only nodes close to a virtual pipe between the source and the sink can forward data. • Number of nodes within the pipe is critical. • Protocol can be initiated by the source or the sink.
DBR [57]	• Hop-by-hop • Demand-based • Flooding	• Each node is equipped with a depth sensor. • Priorities are given to forwarding nodes according to depth differences. • Does not need any network information. • Uses multiple sinks for high packet delivery rate.
HydroCast [58]	• Hop-by-hop • Demand-based • Hierarchical • Network state	• Nodes are equipped with depth sensors. • Local clusters are formed to assign priorities to forwarding nodes according to their depths. • Each node keeps a recovery route. Localization is performed by a centralized monitor, to which nodes send their coordinates periodically. • Multiple sinks are used for packet delivery.

Table 4.2 (cont'd)

Protocol	Classification	Remarks
DFR [59]	• Hop-by-hop • Demand-based • Geographical	• Controlled packet flooding in conformity with link quality, provided that nodes can measure it via propagation delay and bit errors. • Every node knows its own position, the locations of its one-hop neighbors, and the location of the sink. • If the link quality is poor, more nodes forward the same packet, causing ineffective use of sources.
VAPR [60]	• Based on [58] • Hop-by-hop • Demand-based • Hierarchical • Network state	• Nodes are equipped with depth sensors. • Based on periodic beacons and information exchange among nodes and multiple sinks. • Uses locations of 2-hop neighbors of each node. • Energy consumption of pressure sensors must be investigated to deal with lifetime issues.
PULRP [61]	• Hop-by-hop • Demand-based • Hierarchical • Network state	• With the sink at the center, the network is divided into concentric spherical layers, radii of which depend on packet delivery ratio and latency. Node density is assumed to remain uniform in each layer. • Layer setup is repeated for every three packets received at the sink. • All nodes transmit at the same and fixed power level in a low-traffic scenario.
QELAR [62]	• Hop-by-hop • Demand-based • Network state	• Based on learning the environment to solve decision problems. • Nodes keep and periodically update the routing information of their one-hop neighbors. The amount of data storage can be critical, depending on node density. • The objective of the protocol is to achieve equal energy consumption at nodes.
SZODAR [63]	• Hop-by-hop • Table-based • Network state	• Aims to prevent loss of connectivity in shadow zones, where the direction of an acoustic signal changes due to refraction. • Each node maintains a routing table via periodic packet exchange. A route setup phase is repeated whenever a node fails to forward a data packet. • Depending on the packet delivery ratio, nodes adjust their transmission power levels and physically relocate their transceivers.
E-PULRP [64]	• Based on [61] • Hop-by-hop • Demand-based • Hierarchical • Network state	• The network is divided into concentric spherical layers around the sink. Node density is assumed to remain uniform in each layer. • Requires a layer maintenance phase, where nodes determine or update their layers. Sizes of the layers are determined by packet delivery ratio and latency. • Uses CDMA MAC with orthogonal spreading sequences for minimizing packet losses due to collision.

Table 4.2 (cont'd)

Protocol	Classification	Remarks
3D Routing [65]	• Hop-by-hop • Demand-based • Network state • Centralized	• Two routing protocols are proposed. • In the delay-insensitive protocol, each node selects its next hop according to energy and packet error rate information. Data exchange is performed with packet trains for channel utilization efficiency. • The delay-sensitive protocol is based on the centralized coordination of the sink.
DUCS [66]	• Hop-by-hop • Demand-based • Hierarchical	• Proposed to solve energy efficiency problem in long term applications which are not time-critical. • Sensor network is divided into clusters in the setup phase. In the second phase, data is collected within the clusters, and packets are forwarded to the sink over cluster heads. • Mobility of nodes can be critical for cluster formation and maintenance.
APCR [67]	• [61] and [64] • Hop-by-hop • Demand-based • Hierarchical • Network state	• Spherical layers are formed around the sink. • Routes are determined according to the layer number and residual energy of each node. • A node increases its transmission power until it finds a forwarding node for a data packet.
CARP [68]	• Hop-by-hop • Demand-based • Network state	• Only nodes with a history of successful packet transmissions are selected as relays. • Requires link quality, residual energy, and hop count information related to one-hop neighbors. • Exploits modem power control to avoid errors.
Mobicast [69]	• Hop-by-hop • Demand-based • Geographical • Mobile geocast	• It is assumed that each node knows its location. • The protocol is designed to gather data at an autonomous underwater vehicle (AUV) or a mobile sink. • The AUV travels a user-defined route and continuously collects data from nodes within a series of 3-D zones. Sensors are allowed to remain in sleep state, and only nodes in the zone near the sink are active. • Timing precision is needed to wake up nodes when the AUV is in their transmission range.

Mostly, routing protocols are demand-based and they operate on a hop-by-hop basis. That is, routes are established on demand when it is required to relay data to the sink, and forwarding decisions are made at each hop. However, there are also few routing solutions that are based on routing tables at nodes [63] or end-to-end route decisions [56], which is rather impractical due to the spatio-temporal uncertainties in the underwater environment [1], [53].

Most of the proposed solutions require either geographical or network state information [54]-[56], [58]-[65], [67]-[69]. It is assumed that every node in the network has its own location information, each node is aware of the locations of its neighbors, and every data source knows

the location of the final destination. Moreover, network information such as link quality, route conditions, or residual energies of nodes can also be utilized at nodes. For example, in [56], a virtual routing pipe is built, and only nodes that are close to this pipe can relay data. Simulations [55] reveal that using location information and changes in node positions yield to failures to deliver packets when nodes have little or no mobility. In addition to using location information, [59] presents a controlled packet flooding technique in accordance with link quality, provided that nodes can measure it via propagation delay and bit errors. The flooding method is utilized to increase routing reliability; however, multiple nodes forward the same packet, leading to packet overhead and congestion. Protocols proposed in [58] and [60] use periodic beacons sent from multiple sinks. Next hop selection is achieved using sequence number, hop count, and depth information exchange among nodes and sinks. These protocols require location information for the 2-hop neighbors of each node. Moreover, nodes must contain special hardware, and energy consumed by the pressure sensor in order to find depth can lead to lifetime issues.

In DBR [57], most of the nodes are active, since data packets are routed greedily towards multiple sinks placed on the water surface. The objective of the protocol is to obtain a trade-off between packet delivery ratio and energy consumption in the network. Nodes do not need network information or synchronization. Instead, the authors suggest equipping every node with a depth sensor to decide route direction. Each node that receives a data packet acts as a relay if its depth is less than that of the sender and if it has not already sent the packet before. Before relaying, the node waits for a holding time that depends on the depth difference between the node and the sender of the packet. Nodes that are closer to the sink wait for a shorter duration to forward data. Thus, a transmission order is determined among nodes through packet holding times; however, collision avoidance is not taken into account for nodes that are at the same depth.

VBF [56] is one of the most-cited protocols which tackle the routing problem for underwater acoustic communications. Event detecting sources forward packets to nodes residing in a constrained virtual pipe towards the sink. The efficiency of the protocol depends on the radius of the pipe, which defines the number of forwarding nodes in the event-to-sink route. Number of required transmissions, interference, collisions, and number of duplicate packets are directly influenced by the density of nodes in the pipe.

4.3 Transport Layer Protocols

Regarding the transport layer, only a few solutions have been proposed. Those solutions discuss the applicability of error control techniques for the selection of links that optimize power attenuation and transmission delay. Details on those studies are presented in Table 4.3.

Table4.3: Transport Layer Protocols for UASN

Protocol	Classification	Remarks
[70]	• ARQ-based • Per-hop • ACK and NACK	• For a specific transmission, all possible candidates for cooperation are determined according to inter-node distances. • A packet is retransmitted from a cooperative node until successful reception at the destination node.

Table 4.3 (cont'd)

Protocol	Classification	Remarks
FOCAR [71]	• ARQ and Fountain coding • Per-hop • ACK and NACK	• Fountain codes and selective repeat are used to achieve low error recovery complexity and to reduce the overall end-to-end delay. • It can be integrated with an on-demand routing protocol to learn the measured packet error rate of each acoustic relay link.
[72]	• ARQ-based • Per-hop • Implicit/Explicit ACK	• A per-hop hybrid ACK scheme for Stop and Wait ARQ in a multi-hop acoustic channel. • If a node transmits a packet and hears its next-hop neighbor transmitting it forward, it is an implicit ACK. • For acoustic links with higher BER, ACKs may be implemented on a per-hop basis.
[73]	• ARQ-based • Per-hop • Implicit ACK	• Packet size is adjusted such that transmission time becomes smaller than propagation delay. Transmissions are scheduled to achieve collision avoidance. • ACK is replaced with packet overhearing after transmission at the next hop.
MPNC [74]	• Based on [85] and [75] • Network coding • Per-hop • Implicit ACK	• Three disjoint data paths are established, and two groups of individually coded packets are transmitted over two side paths. A joint set of the two groups is transmitted over the third path. • A node overhears packets from its upstream and downstream neighbors.
IPool-ADELIN [75]	• Based on [76] • Per-hop • FEC • BCH codes and Erasure coding • Implicit ACK	• Data packets are ACKed implicitly by overhearing at the corresponding sender. • Local link maintenance is achieved through FEC and coding when the bit error rate of the monitored link is high. • Achieves higher data delivery ratio and lower energy consumption than [76].
ADELIN [76]	• FEC and binary BCH code • Per-hop	• Uses combinations of FEC and BCH coding. • Regardless of the required number of packets, all encoded packets are transmitted, yielding to high end-to-end delays in multi-hop operation [77].
FRT [77]	• FEC-based • Per-hop • ACK and NACK	• Uses FEC and link quality information at each hop. • The number of packets to be transmitted is determined according to link quality, which is the ratio of the number of received encoded packets to the number of transmitted packets.
ARRTP [78]	• Redundancy • Per-hop • BCH and Reed-Solomon codes • Distance-based	• BCH is used for bit-level FEC. • Reed-Solomon codes are preferred for packet level erasure coding at various inter-node distances. • A packet is retransmitted from a cooperative node until successful reception at the destination node.

Table 4.3 (cont'd)

Protocol	Classification	Remarks
RTS [79]	• Fountain coding • Per-hop • ACK and NACK	• For uniform data reliability in the sensing zone, a distributed storage scheme with concatenated fountain codes is designed. • Multiple acknowledgments guarantee the reliability of control messages.
M-FEC [80]	• FEC and Hamming coding • End-to-end	• In the intermediate nodes, Hamming Coding recovers some corrupted segments. At the destination, all received packets are corrected by the decoder, and packets from different paths are combined into the original packet using M-FEC. • A decision and feedback method is exploited in the receiver to decrease the number of relay paths.
LAA [81]	• Aggregation of ACKs • End-to-end • Location information	• Each node knows its own location and its neighbors' locations. The sink is aware of the locations of sources. • The sink aggregates ACK packets for the corresponding data sources, and transmits the aggregated ACK with the addresses of source nodes.
UW-HARQ [82]	• FEC and ARQ • End-to-end • ACK and NACK	• In ARQ, NACK packets inform the source about the number of packets to retransmit, and ACK packets indicate the success of packet recovery at the receiver. • Number of retransmissions is minimized by using an adaptive coding ratio estimation method.
SDRT [83]	• FEC and ARQ • Per-hop • Erasure coding • Explicit ACK	• Erasure codes are used for per-hop data transfer. A data block is decoded, reconstructed, encoded, and transmitted at each hop. • The sender continues to transmit encoded packets until it receives a positive ACK, causing high energy consumption.
[84]	• RFEC and ARQ • Per-hop • Explicit ACK	• The protocol uses Random FEC to deal with high bit error rate, and ARQ to avoid frequent feedbacks. • Receiver sends an ACK to sender only when it receives all of the transmitted packets.
[85]	• Network coding • Per-hop	• Before transmission, a node encodes several packets into one or more outgoing packets. • Two schemes are proposed to improve the efficiency of network coding. One scheme adjusts routing paths, whereas the other modifies the redundancy on each node. • Packet recovery is performed at the receiver by using network coding.

Table 4.3 (cont'd)

Protocol	Classification	Remarks
[86]	• Biologically inspired • Per-hop • Congestion control solution	• Congestion control mimics the abilities of marine communities to deal with population explosion and to move the system back to equilibrium. • A mathematical model is developed to determine the growth rate of data at nodes in terms of CPU capacity, buffer levels, and system parameters. • Proposed and analyzed for a tree topology, in which each node has at most two children. • Performance can be degraded by node mobility.

Protocols that are based on Automatic Repeat Request (ARQ) aim to achieve error control by using acknowledgments (ACKs) and timeouts [70]-[73]. A sender retransmits a packet unless it receives an ACK, indicating successful packet delivery at the receiver. ARQ-based solutions suffer from long propagation delay, packet traffic, and high energy consumption due to retransmissions.

To reduce packet overhead, implicit ACKs can be deployed [72]-[75]. With this approach, if a sender overhears the transmission of the same packet from its next-hop neighbor, it interprets this as an ACK.

To avoid the limitations caused by the feedback mechanism in ARQ, Forward Error Correction (FEC) techniques are exploited [75]-[79]. Successful recovery of received packets at the receiving node significantly affects the overall packet error rate and the number of multiple paths required for data delivery. In order to perform error control coding, protocols use BCH, fountain, erasure, Hamming, or Reed Solomon codes together with network information such as link quality, required number of packets, inter-node distances.

Hybrid protocols [80]-[84], benefit from the advantages of both ARQ and FEC. Retransmission overhead in ARQ is decreased by informing the sender about the required number of transmissions via negative ACK (NACK) messages. Besides, packet recovery is achieved through low-complexity linear coding methods at the receiver. While most of the proposed solutions operate on a per-hop basis, hybrid protocols try to achieve end-to-end reliability through ACK aggregation, adaptive coding ratio estimation, or ACK-NACK message exchange.

Network coding is utilized by [85] and recently by [74] to improve recovery efficiency. Before transmission, a node encodes several packets into one or more outgoing packets. Individually coded packets are transmitted over disjoint data paths to enhance the chance of successful recovery at the receiver.

Recently, [86] is a biologically-inspired congestion control solution, which imitates the behavior of marine communities in dealing with population equilibrium. A mathematical model is developed to determine data growth at nodes in terms of CPU limits, buffer levels, and required system parameters. Since the protocol is proposed and analyzed for a tree topology, its performance must be investigated under different deployments and with changing mobility levels.

In the next chapter, we present a cross-layer protocol for RPUASN powered by the sink, considering the channel characteristics and communication requirements studied in Chapters 2 and 3.

CHAPTER 5

CROSS LAYER POWER ADAPTIVE CSMA/CA FOR SPUASN

''Truth is ever to be found in the simplicity, and not in the multiplicity and confusion of things.''
Sir Isaac Newton

The term Sink Powered Underwater Acoustic Sensor Networks (SPUASN) refers to a special configuration within the recent RPUASN paradigm, where the data sink supplies power to battery-free sensors that constitute the network. In this chapter, we introduce the Cross Layer Power Adaptive CSMA/CA (X-PACCA) protocol for SPUASN. With the traditional lifetime constraints alleviated, X-PACCA integrates MAC, network, and transport layer functionalities. Packet relaying/routing is based on CSMA/CA backoff window size adjustment according to harvested power levels at nodes. End-to-end reliability is enhanced via acknowledgments sent by the sink. Congestion is avoided via prevention of redundant packet forwarding. Neither global network information nor synchronization is required at nodes. It is shown that, with appropriate selection of protocol parameters, X-PACCA achieves low end-to-end latency and high packet delivery performance.

5.1 Introduction

For the collaborative operation of SPUASN nodes deployed in a volume powered by the sink, it is imperative that sensed event information is reliably transferred over multiple hops by exploiting the shortest path to the data sink. We introduce the X-PACCA protocol for SPUASN, integrating MAC, network, and transport layer functionalities. It is based on the determination of initial backoff window sizes to be used for packet transmission and relaying, according to harvested power levels at nodes. To resolve contention at relay nodes, SPUASN nodes are prioritized by using the difference between the power levels at the transmitter and the receiver of a packet. Access priorities are given to nodes closer to the sink, resulting in a loop-free path to reduce end-to-end packet delay. While waiting for medium access to transmit a packet, if a node hears the successful forwarding of the packet by another node, it cancels the transmission. Thus, congestion is avoided via prevention of redundant packet forwarding at nodes that receive the same date packet. Finally, end-to-end reliability is enhanced via acknowledgments sent by the sink upon reception of packets. X-PACCA does not require global network information or clock synchronization at nodes; protocol operation proceeds via local decisions of individual nodes based on harvested power levels.

The remainder of the chapter is organized as follows. The operation of the X-PACCA protocol

is described in Section 5.2. Performance evaluation of X-PACCA and comparison to some available alternatives in terms of end-to-end delay, packet delivery ratio, and packet receiving throughput is presented in Section 5.3. Section 5.4 concludes the chapter.

5.2 Protocol Description

X-PACCA is responsible for the following MAC, network, and transport layer functions:

- Organizing the access of SPUASN nodes to the shared medium.

- Routing of data packets along a path from the event region to the sink.

- Congestion avoidance through prevention of redundant packet forwarding in case of multiple nodes relaying the same packet.

- End-to-end reliability enhancement via ACKs sent by the sink.

Using the relations given in Chapter 2, a node knows its power budget harvested from the sink, P_{harv}. The transmission power level of the omnidirectional communication transducer of a node is a portion of the harvested power level, and it is denoted as $MYPL = \beta P_{harv}$ ($0 < \beta < 1$). Each node has a unique identifier (ID), denoted by $MYID$.

Each node maintains the following queue structures:

- A MAC Transmit Queue (MTQ), holding packets to be transmitted and operating according to CSMA/CA with a unique starting window size for each node.

- A list (IGS) of packets to be ignored (already processed and/or relayed by the SPUASN node), used to store the IDs of packets ($PIDs$) that must not be re-processed or re-relayed. If PID is already a member of IGS, the list is not modified upon re-insertion.

- A list (WFA) of data packets waiting for ACK together with their detection times, maintained only at event data source nodes.

The format for X-PACCA data packets is shown in Fig. 5.1. A single bit $TYPE$ field is used to identify packets sent by the sink. SID represents the ID of the data source node that has sensed an event, and $EVID$ is the sequence number of the sensed event, which is repeated in a sufficiently long time for sensor network data pipeline capacity. These two fields form the packet ID, $PID = SID + EVID$. The transmission power level (TPL) is the power level with which the packet was transmitted, either from the original sensing node or when relayed. Event data necessary for the application level is carried in the $PAYLOAD$ bits, and CHK contains the checksum bits for error detection and correction.

The operation of X-PACCA upon event sensing is given in Algorithm 1. A node that senses an event constructs a packet with $PID = MYID + EVID$, $TPL = MYPL$, $TYPE = 0$, filling the corresponding $PAYLOAD$ and CHK fields. It inserts the packet into MTQ, and starts CSMA/CA transmission, applying the backoff procedure as given in Algorithm 3, with a fixed initial backoff window size W_s. Hence, regardless of where an event is sensed, the data source

TYPE	SID	EVID	TPL	PAYLOAD	CHK

Figure 5.1: X-PACCA data packet format

node gets a fair chance for medium access. After successful transmission, the packet is deleted from MTQ, the node enters PID and local timestamp value into WFA, and PID is inserted into IGS, meaning that the node has processed the packet. Thus, if the node hears the same packet again from a neighbor, it simply discards the newly arrived copy.

The node periodically checks the ($PID, timestamp$) pairs in WFA, and those still unacknowledged after WFA_{thresh} are re-sent in case the corresponding event $EVID$ is still active. Otherwise, the pair is deleted from WFA queue.

The behavior of a node upon packet reception is presented in Algorithm 2. When a node receives a packet with $TYPE = 1$, that is an ACK coming from the sink, PID is searched and removed, if found, from WFA. The node also deletes PID from MTQ if found, and cancels pending CSMA/CA if not yet completed, because there is no need to relay a packet that has already been received successfully by the sink. Outdated packets are removed from the queues eventually to avoid indefinite growth of queue size; however, PID is not erased from IGS immediately. Instead, the node keeps PID in IGS for another duration of D, which is the propagation delay of the longest hop in the network. Hence, duplicate forwarding is avoided in case delayed packet arrivals occur from other neighbors.

When an SPUASN node receives a packet from any neighbor ($TYPE = 0$), the node compares its own transmission power level ($MYPL$) with that (TPL) of the sender of the packet. If

---

Algorithm 1 X-PACCA pseudo-code for event sensing

```
 1: procedure EVENTSENSED(EVID)
 2:     pkt = CreatePkt(0, MYID, EVID, MYPL, payload, chk)
 3:     MTQ.insert(pkt)
 4:     Backoff(Wₛ, pkt)                                      ▷ CSMA/CA backoff, initial window size Wₛ
 5:     MTQ.delete(pkt)
 6:     WFA.insert(pkt.PID, timestamp(EVID))                              ▷ Wait for ACK
 7:     IGS.insert(PID)                          ▷ If you hear this event again, do not relay packets
 8:     while WFA is not empty do                       ▷ WFA is checked for ACK from the Sink
 9:         for all PID ∈ WFA do
10:             if myClock ≥ WFA.timestamp(EVID) + WFAₜₕᵣₑₛₕ then
11:                                                                        ▷ No ACK has arrived yet
12:                 if SenseEvent(EVID) then
13:                                                           ▷ The event is still active; re-transmit
14:                     pkt = CreatePkt(0, MYID, EVID, MYPL, payload, chk)
15:                     MTQ.insert(pkt)
16:                     Backoff(Wₛ, pkt)
17:                     MTQ.delete(pkt)
18:                     WFA.update(pkt.PID, timestamp(EVID))
19:                 else                                              ▷ The event is not active anymore
20:                     WFA.delete(pkt.PID, timestamp(EVID))
21:                                                                        ▷ Do not re-transmit
22:                 end if
23:             end if
24:         end for
25:     end while
26: end procedure
```

Algorithm 2 X-PACCA pseudo-code for packet reception

```
1:  procedure PACKETRECEIVED(pkt)
2:      if pkt.Type == 1 then                                              ▷ Sink packet
3:          if WFA.find(pkt.PID) == TRUE then                             ▷ Check WFA
4:              WFA.delete(pkt.PID, time(pkt.EVID))                  ▷ ACKed; do not wait
5:          end if
6:          if MTQ.find(pkt.PID) == TRUE then                            ▷ Check MTQ
7:              MTQ.delete(pkt.PID)                             ▷ Cancel retransmission
8:          end if
9:          if IGS.find(pkt.PID) == TRUE then                            ▷ Check IGS
10:             IGS.scheduleDelete(pkt.PID, D)
11:                                               ▷ Delete PID from IGS at currentTime + D
12:         end if
13:     else                                        ▷ Packet from a relay node, pkt.Type = 0
14:         if IGS.find(pkt.PID) == FALSE then                 ▷ I have not processed this pkt
15:             IGS.insert(pkt.PID)
16:             if pkt.TPL < MYPL then                    ▷ Closer to the sink; may relay pkt
17:                 pkt.TPL = MYPL                               ▷ Update pkt.TPL field
18:                 MTQ.insert(pkt)                        ▷ Packet waiting for transmission
19:                 W_min = k/(MYPL − pkt.TPL)              ▷ Initial backoff window size
20:                 Backoff(W_min, pkt)
21:                 MTQ.delete(pkt)
22:             else                          ▷ Packet relayed by a node closer to the sink
23:                 if MTQ.find(pkt.PID) == TRUE then
24:                     MTQ.delete(pkt.PID)                       ▷ Cancel retransmission
25:                 end if
26:             end if
27:         end if
28:         if MYID == SinkID then                                       ▷ I am the sink
29:             pkt.Type = 1                            ▷ ACK broadcast from the sink
30:             BroadcastPkt(pkt)
31:         end if
32:     end if
33: end procedure
```

$TPL < MYPL$, the packet is coming from a neighbor that is further from the sink, and the node may relay the packet. It ignores the packet if $PID \in IGS$, showing that it has processed and/or relayed the packet before, and this is a duplicated arrival. Otherwise, the node must relay the packet with $TPL = MYPL$ update, and it enters PID into IGS and MTQ.

To minimize end-to-end delay, nodes closer to the sink have a higher priority to access the medium for relaying packets. Hence, at relay nodes, the initial backoff window size is adapted according to the power differential between the previous sender and this relay node, and determined as $W_{min} = k/(MYPL − TPL)$. Effects of the choice of the backoff constant k on performance is investigated in Section 5.3. Then, the node starts exponential backoff, as detailed in Algorithm 3. The flowchart of the backoff mechanism in X-PACCA is depicted in Fig. 5.2. When CSMA/CA does succeed in transmission (i.e., no collision) after backoff, the nodes deletes PID from MTQ.

If $TPL \geq MYPL$ for the received packet, this means the node is hearing a packet relayed ahead of itself, from a node closer to the sink. The node inserts PID into IGS if $PID \notin IGS$. The packet has already been relayed by a node closer to the sink, so there is no need to relay a duplicate. The node cancels the pending backoff or transmission procedure for that packet and removes it from MTQ.

Whenever a packet is received at the sink, it is acknowledged by simply setting the $TYPE$ bit and broadcasting it, using W_s as the starting window size. That is, we are assuming that, as the sink can supply power to all sensors in a single hop, the sink can also be heard by all

Algorithm 3 X-PACCA backoff algorithm

```
1:  procedure Backoff(W, pkt)
2:      i = 0                                                        ▷ Backoff stage
3:      txFlag = 0                                                   ▷ Transmission flag
4:      txAttempts = 0                                              ▷ Number of transmission attempts
5:                                              ▷ maxAttempts is the maximum number of attempts
6:      while txFlag == 0  &&  txAttempts ≤ maxAttempts do
7:          txAttempts = txAttempts + 1
8:          Wᵢ = 2ⁱW                                                ▷ Window size, stage i
9:          cnt = unif(0, Wᵢ − 1)                                   ▷ Counter
10:          while cnt ≠ 0 do
11:              repeat
12:                  if MTQ.find(pkt.PID) == FALSE then
13:                      EXIT
14:                                  ▷ Someone else has already transmitted the packet, so cancel transmission
15:                  end if
16:              until channel idle for a slot time
17:              cnt = cnt − 1                                      ▷ Decrement counter
18:          end while
19:          TransmitPkt(pkt)                                       ▷ Forward packet
20:          if collision then
21:              if i ≠ maxBackoff then                             ▷ Maximum backoff stage check
22:                  i = i + 1
23:              end if
24:          else
25:              txFlag = 1                                         ▷ Transmission successful
26:          end if
27:      end while
28: end procedure
```

sensors in a single hop. Hence $TYPE = 1$ packets are not relayed, they simply cause sensors to drop acknowledged packets from their transmission lists.

START

Packet Ready in MTQ

i = 0
W_{min} = k / (MPL − TPL)
txFlag = 0
txAttempts = 0

i = m?

No

Yes

i = i + 1

txFlag = 0 AND
txAttempts ≤ maxAttempts
?

Yes

No

txAttempts = txAttempts + 1
$W_i = 2^i W_{min}$
cnt = unif (0,W_i−1)

WAIT SLOT

Packet still
in MTQ?

No

Yes

Channel idle for a
slot time?

No

Yes

COUNTDOWN

cnt = cnt − 1

cnt = 0
?

No

Yes

TRANSMIT PACKET

collision?

Yes

No

txFlag = 1
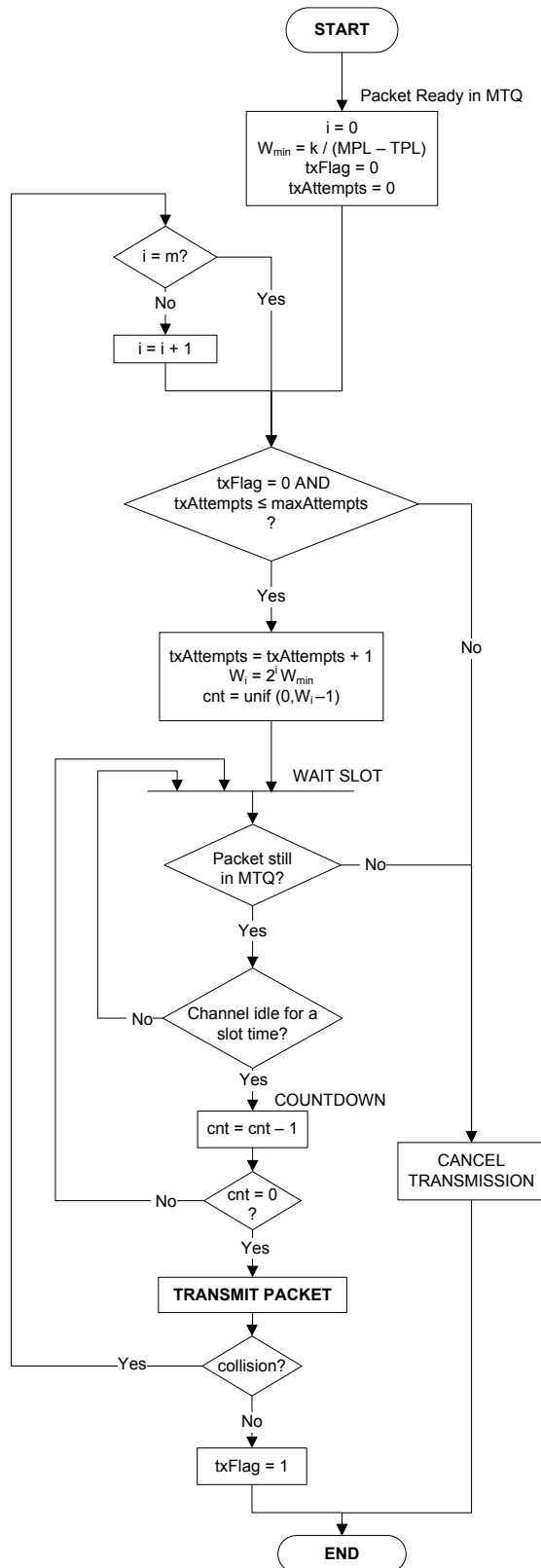
CANCEL
TRANSMISSION

END

Figure 5.2: The flowchart of the backoff mechanism in X-PACCA

46

5.3 Performance Evaluation

In this section, the performance of X-PACCA is evaluated in terms of design parameters and compared with other protocols that have been proposed for underwater sensor networks. Namely, MAC performance of X-PACCA is compared with UWAN-MAC [36] and Slotted FAMA [33], and the routing performance is compared with DBR [57] and VBF [56].

5.3.1 Simulation Settings

All simulations are performed using Aqua-Sim [87], which is a network simulator for underwater sensor networks. Aqua-Sim has the ability of simulating underwater environment for three-dimensional network deployment and implemented as a patch over NS-2 [88], [89]. It adopts a realistic model of the underwater acoustic channel, including multipath effects, time-varying delay, attenuation, and Doppler scaling. The validity of the channel modeled in Aqua-Sim is verified through comparisons with real testbed results [87].

As explained in Chapter 4, MAC protocols for UASN can be classified into two main groups. The operation of the protocols in the first group depends on CSMA and its variations, whereas the second group is composed of reservation-based protocols. Therefore, we selected two most-cited protocols, namely UWAN-MAC and Slotted FAMA, representing each group. As for the routing protocols, we chose two distributed, hop-by-hop, and demand-based protocols, VBF and DBR, which can operate with a single sink, and do not rely on network information or node hierarchy. Due to the stated characteristics of the two protocols, they appear to be among the most appropriate choices for our performance evaluation. All of these protocols have already been implemented and tested in Aqua-Sim [90], hence, our comparative discussions and simulations are based on validated performance results.

Unless otherwise stated, default values for X-PACCA and SPUASN node parameters are given in Table 5.1 and Table 5.2, respectively.

In all simulations, the sink is the external acoustic power source placed at the water surface with the input power of $P_{elec} = 10$ kW, operating at the frequency $f_s = 10$ kHz with an electro-acoustic power conversion efficiency of $\eta = 0.5$. We assume that the level of harvested power is constant during packet transmission at each node, as the sink continues to supply energy in an uninterrupted fashion. Communication frequency among nodes is set to 25 kHz

Table5.1: X-PACCA Protocol Parameters

Parameter	Default Value
Data sink/source starting window size (W_s)	3
Maximum backoff stage (*maxBackoff*)	5
Maximum number of retransmissions (*maxAttempts*)	5
ACK waiting time (WFA_{thresh})	20 s
Ignore timeout (D)	50 s
Aqua-Sim receive threshold	8.7×10^{-8} W

Table5.2: SPUASN Node Parameters

Parameter	Default Value
Required power for a node to operate (P_{req})	0.5 W
Number of harvesting hydrophones (n)	5
Receiving voltage sensitivity (RVS)	-150 dB re V/μPa
Hydrophone impedance (R_p)	125 Ω
Harvesting efficiency	0.7

at a bit rate of 10 kbps. Spherical spreading is assumed for acoustic signals. Infinite queue size has been assumed at the nodes.

Unless explicitly stated otherwise, simulations are repeated until all reported average end-to-end delay (latency) values are within ±10% confidence interval of the actual value with a confidence level (i.e. probability) of 99%. The packet delivery probabilities, however, simply reflect the ratio of successfully delivered packets that constitute the basis for the reported average latencies. That is, in conformance with the commonly accepted convention in networking literature, the statistical confidence of the reported packet loss characteristics are not assessed, as obvious from the relatively inconsistent nature of those results. The consistency of the delay characteristics, however, are taken to be sufficient for an overall evaluation of the performance of the proposed protocol.

Fig. 5.3 shows the topology for the default simulation parameters. As can be seen from the figure, a spherical cone shaped network is formed and nodes, randomly distributed in the medium and satisfying minimum harvested power requirement, are actively participating the network.
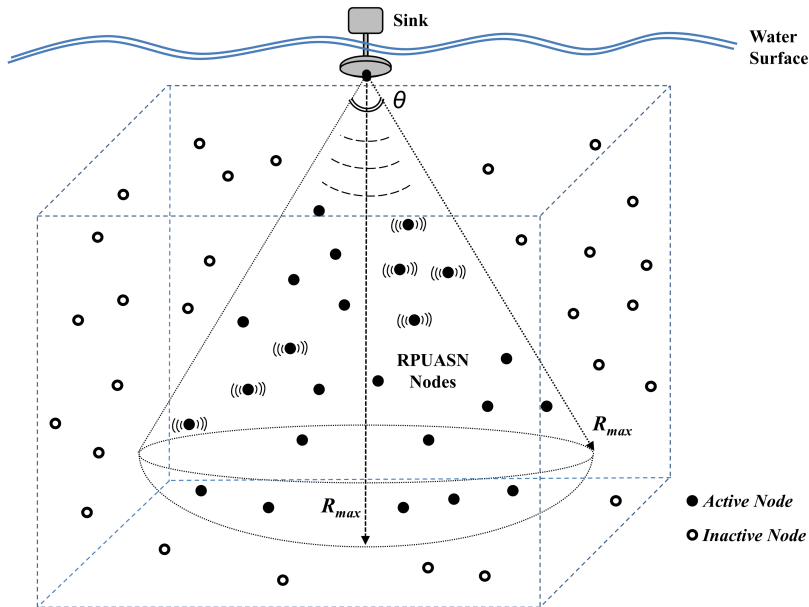
Figure 5.3: Spherical cone deployment for SPUASN

5.3.2 Impact of Design Parameters

First, the impacts of network and protocol parameters over the performance of X-PACCA are examined.

5.3.2.1 Slot Length

Slot length is one of the most crucial parameters in terms of delay and throughput. Fig. 5.4(a) and 5.4(b) show delay and packet delivery probability for a single 600 B packet over an SPUASN with an average number of 60 active nodes. In this case, a single source is placed at a farthermost point to the sink, which is 777 m for a vertex angle of $\theta = 20°$ and $P_{elec} = 10$ kW sink power. Nodes continue retransmitting until successful delivery.
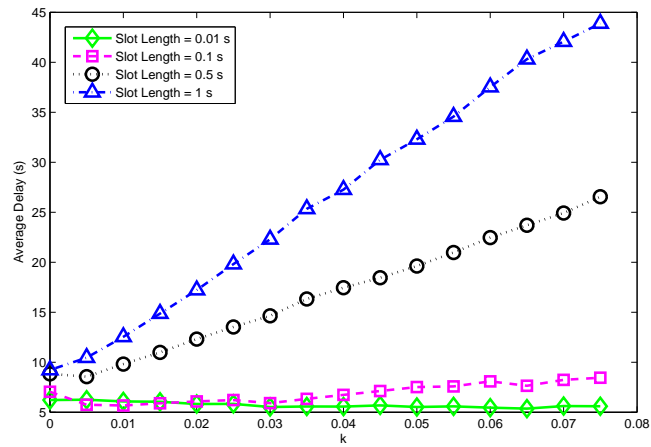
(a) Average delay
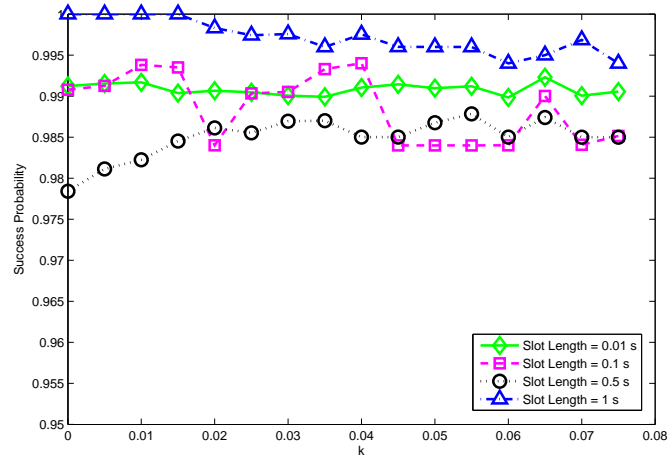
(b) Packet delivery ratio

Figure 5.4: Variation of X-PACCA performance with slot length and backoff constant

Shorter slot lengths reduce the performance by increasing the probability of collision and longer slot lengths cause longer delays. Decreasing the slot length decreases observed delays until a

point where collisions begin to dominate. Fig. 5.4 shows that the effect of k diminishes with shorter slot lengths.

5.3.2.2 Density of Nodes

Effect of node density, again on end-to-end delay and delivery ratio, is investigated for different values of the backoff constant, k.
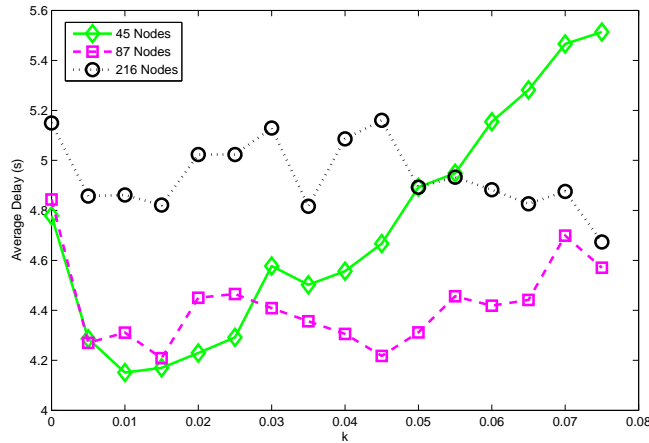
(a) Average delay
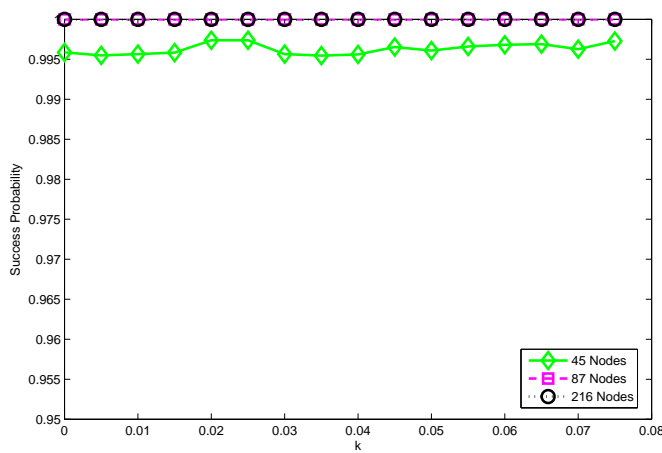
(b) Packet delivery ratio

Figure 5.5: X-PACCA performance with backoff constant and node population

Data source node is placed at the farthermost point to the sink, which is 535 m away for $\theta = 30°$ and $P_{elec} = 10$ kW. At each run, a 600 B packet is transmitted from the data source to the sink. Packets are retransmitted until no collision occurs; however, the maximum backoff stage is $maxBackoff = 5$, as stated in Table 5.1. According to the results depicted in Fig. 5.4, slot length in the backoff is taken as 0.1 s.

Fig. 5.5(a) shows that the choice of k has a more critical effect on end-to-end delay for low node densities, but proper selection of this constant leads to lower latencies. Higher sensor

densities also result in higher packet delivery ratio as expected, as can be seen in Fig. 5.5(b). However, packet delivery ratio is very close to 100% for all investigated node densities.
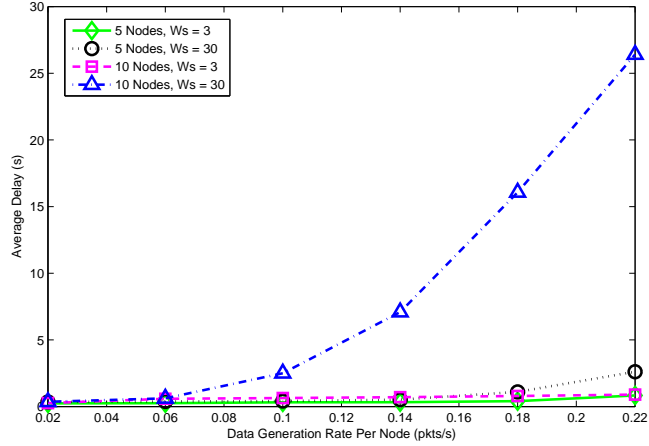
(a) Average end-to-end delay
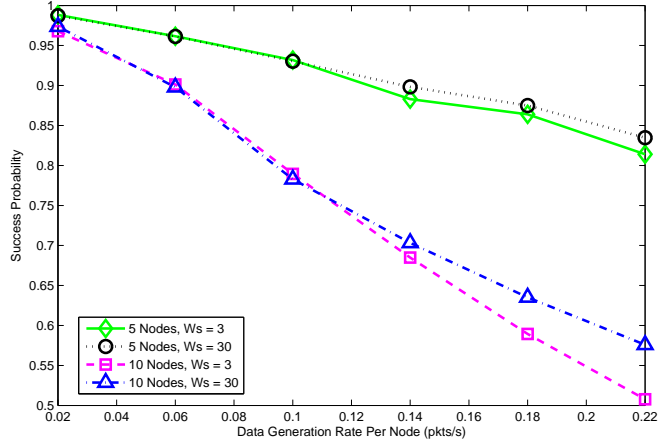
(b) Packet delivery ratio

Figure 5.6: Performance of X-PACCA for different W_s

5.3.2.3   Effect of Source Window Size (W_s)

A spherical cone shaped topology is formed by the acoustic source as a result of $\theta = 20°$ and $P_{elec} = 10$ kW. In the simulations, 5 and 10 source nodes are deployed randomly inside this cone such that all sources can deliver packets to the sink in a single hop. All nodes other than the sink are data sources and send 50 B packets with independent but identically distributed Poisson traffic. Backoff constant $k = 1$ and $\beta = 0.025$ guarantees single hop access to the sink, according to the range that directly depends on the transmission power (as discussed in Chapter 2) and the Aqua-Sim receive threshold [87] given in Table 5.1. Slot length is 0.005 s. To avoid congestion from multiple sources, the maximum number of transmission attempts is limited to *maxAttempts* = 5, as given in Table 5.1.

Fig. 5.6(a) and Fig. 5.6(b) show latency and delivery ratio values for different source window

51

sizes and different average number of source nodes, respectively. As can be seen from these figures, small window sizes result in better performance at low traffic rates, whereas larger window sizes are needed with higher traffic rates.
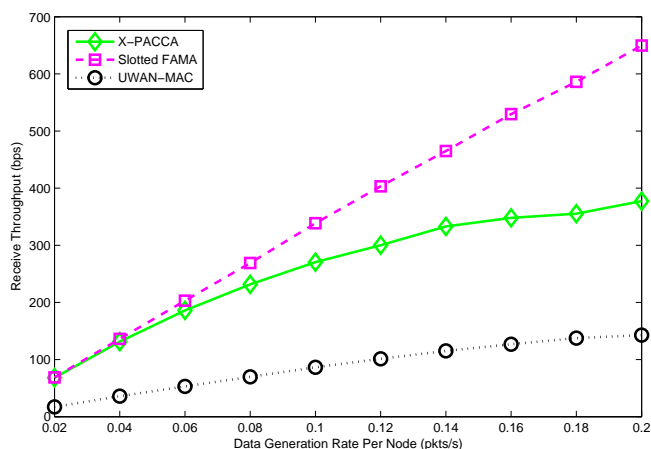
(a) Throughput
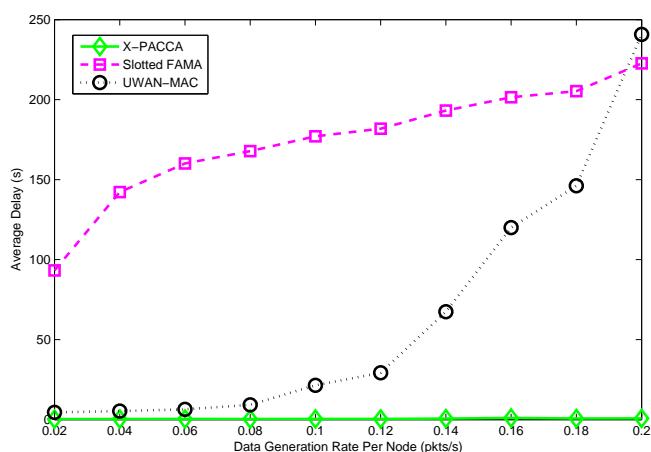
(b) Delay

Figure 5.7: Comparison of MAC performance of X-PACCA with related protocols

5.3.3 Comparison of MAC Performance

MAC performance of X-PACCA is compared with UWAN-MAC [36] and Slotted FAMA [33] in terms of throughput and delay. To get rid of routing effects, network configuration is set such that transmitted packets can reach the sink in a single hop. A spherical cone shaped topology is formed by the acoustic source with $\theta = 30°$ and $P_{elec} = 10$ kW. An average of 9 active nodes are randomly placed inside this cone, and packet size used is 50 B.

X-PACCA slot length is set to 0.005 s and $k = 0.1$. β is set to 0.025 to satisfy single hop requirement of this simulation. Maximum backoff stage for Slotted FAMA is set as 15, and maximum burst is taken as 30. Average and deviation of cycle period parameters used in UWAN-MAC simulations are 1 and 0.1, respectively.

Fig. 5.7(a) shows the receive throughput and Fig. 5.7(b) shows the delay obtained with all three protocols. As can be seen from figures, UWAN-MAC achieves lower throughputs and higher delays at high packet generation rates compared to the other two protocols. This is an expected result of duty cycling applied in UWAN-MAC, which primarily aims to enhance energy efficiency. In UWAN-MAC, two different nodes might have the same transmitting period resulting a collision, so when traffic rate increases, collisions dominate and throughput will no longer increase. Slotted FAMA and X-PACCA have similar throughput levels at low packet generation rates, but when this rate increases Slotted FAMA achieves better throughput as a result of its RTS/CTS handshaking mechanism and trains of packets technique (burst of packets sent with a single handshake). RTS/CTS mechanism in Slotted FAMA decreases collision probability hence results in better throughput values but significant delays in packet transmissions can be observed when compared with X-PACCA.

To sum up, UWAN-MAC, which is recommended mainly for delay-tolerant applications, favors energy efficiency and has lower throughput and high delay at high traffic rates. X-PACCA and Slotted FAMA display similar throughput results at low packet generation rates; but when this rate increases, the effect of collisions lowers throughput values of X-PACCA. On the other hand, X-PACCA performs much better than both others in terms of delay.

5.3.4 Comparison of Routing Performance

In this set of simulations, packet delivery ratio and average end-to-end (E2E) delay values of X-PACCA are compared with DBR [57] and VBF [56]. The scenario used for simulations is the same as that in [57] except for the topology, operating X-PACCA in a spherical cone shaped geometry, as shown in Fig. 5.3. All simulations last for 5000 s with 50 packets and each data point is a result of 20 simulations (average of 1000 packets). Slot length is 0.005 s, k = 0.001, and packet size is 50 B.

Transmission ranges in DBR and VBF simulations are fixed for all nodes and set as 100 m. In X-PACCA, transmission ranges are proportional to the power harvested by each node, as discussed in Chapter 2. Using P_{elec} = 10 kW and $\theta = 30°$ for the sink with $\beta = 0.0007$ at the nodes, the average transmission range of nodes in X-PACCA is $r_t = 95$ m, which is slightly less than the fixed transmission range used in DBR and VBF - i.e., favoring DBR and VBF at the expense of X-PACCA. The values of k and β used in this simulation guarantee multi-hop operation within the volume of deployment.

Average E2E delay and packet delivery ratio performances are plotted in Fig. 5.8(a) and Fig. 5.8(b), respectively. Since SPUASN nodes have different transmission ranges increasing with power harvested by node, X-PACCA can send via a smaller number of hops which means smaller delays. X-PACCA also performs best in terms of packet delivery ratio when compared with single sink simulations. Only multi-sink DBR performs better at low number of nodes.

5.3.5 Cross Layer Performance of X-PACCA

Finally, we present the latency and delivery success performance achieved when MAC, relay and transport layer functionalities are collectively effective. In the simulations for each data point shown in Figure 5.9a and 5.9b, out of a total of 1200 randomly placed nodes, an average of 200 or 400 were within the spherical cone receiving energy from the sink. The electrical
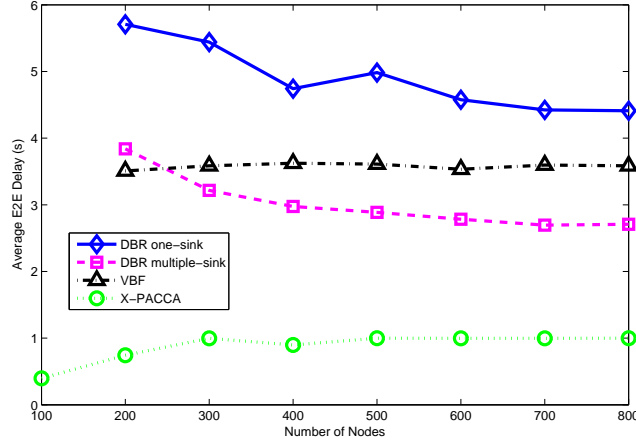
(a) Average end-to-end delay
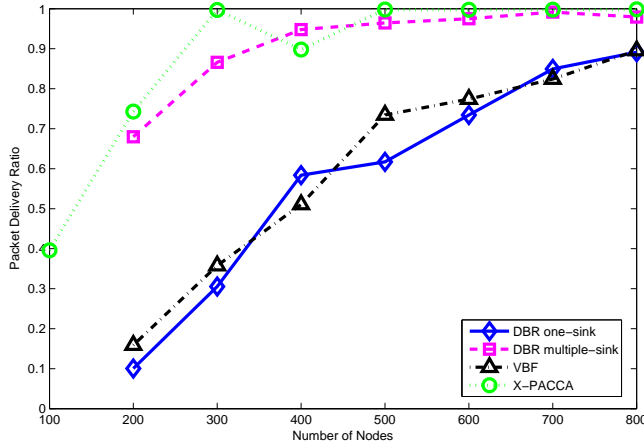
(b) Packet delivery ratio

Figure 5.8: Comparison of routing performance of X-PACCA with DBR and VBF

power at the sink was $P_{elec} = 10$ kW and $\theta = 30°$, resulting in $R_{max} = 535$ m as the depth of this cone. 20 or 40 data source nodes randomly selected with equal probability among these were generating Poisson traffic of 50 B packets, contributing to the total packet generation rates depicted in the figures. As in the previous subsection, assuming $\beta = 0.0007$ gives an average transmission range of 95 m at nodes. Each simulation was repeated until the latency results were within the targeted level of confidence. X-PACCA slot length was taken as 0.005 sec, and the backoff constant was $k = 0.001$. The assumed values of k and β enable multi-hop operation, as in the case of routing performance evaluation of X-PACCA. It is shown in Fig. 5.6 that increasing the starting window size helps in resolving the contention which results from adding more sources to the network. Therefore, W_s was set to 30 to maintain a high success probability when the number of sources is changed between 20 and 40.

With the investigated configuration, packets generated by 40 sources are delivered over a maximum distance of 535 m with a delay less than 2 s, at a delivery ratio more than 80%. Populations of 200 and 400, as analyzed in Chapter 2, are above the minimum number of
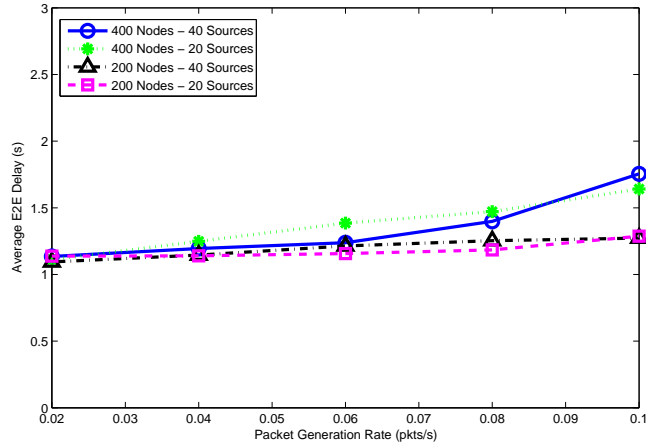
(a) Average end-to-end delay
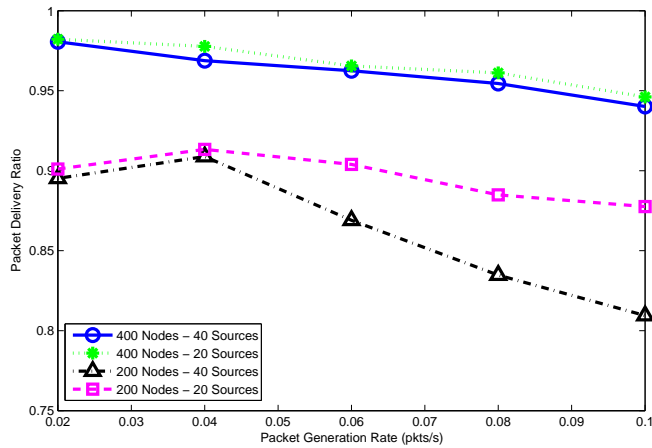
(b) Packet delivery ratio

Figure 5.9: Cross layer performance of X-PACCA in terms of latency and delivery ratio

sensors to achieve 1-coverage in the given volume, and hence, even better performance may be obtained with networks of sparser populations.

5.4 Conclusion

We have presented a new, cross-layer, power adaptive CSMA/CA (X-PACCA) protocol that caters for MAC, routing and transport layer needs of sink powered underwater acoustic sensor networks. For packet relaying and routing, the protocol exploits differences of the level of power harvested at sensors according to their distance from the data sink which is also the remote supplier of acoustic energy. MAC layer operates according to CSMA/CA rules, and transport layer reliability is achieved through packet acknowledgment by the data sink. Duplicate forwarding, while possible, is effectively suppressed by individual relays dropping packets as soon as relay from a more powerful node, i.e. one that is closer to the sink, is detected.

Sink acknowledgments cause not only original data sources to avoid repeated transmission of event information, but also permit intermediate relays to cancel any pending forwarding of already received packets. It is shown that appropriate selection of protocol parameters ensure acceptable latency, throughput, and delivery performance.

CHAPTER 6

CONCLUSION

''However beautiful the strategy, you should occasionally look at the results.''

W. Churchill

This chapter includes some concluding remarks related to the ideas presented and discussed in this study. The contributions of the thesis are outlined and possible future work directions are summarized.

6.1 Contributions

The major contribution of this thesis is two-fold : (1) RPUASN solution to achieve indefinite lifetime in underwater acoustic communication networks; and (2) X-PACCA protocol for power adaptive SPUASN communications. In addition to introducing the RPUASN model and proposing X-PACCA, this study also discussed the channel capacity in RPUASN and presented an extensive and categorized literature survey on the communication protocols proposed for UASN.

6.1.1 RPUASN Paradigm

We introduced *RPUASN* as a novel paradigm to remove the challenge on the lifetime of UASN. Power harvesting from various sources have been discussed in the literature [8], however, no work has addressed the power requirements of UASN specifically before. This is also validated by the recent survey [91] conducted by *METUTECH Technology Transfer Office (TTO)* and *Yalçıner Patent ve Danışmanlık Ltd. Şti.*. In the survey, several local and international databases [92]-[96] are scanned for any studies or patents related to power harvesting in underwater communication networks. The survey results show that no other work has attempted to solve the energy constraint and limited lifetime problems in UASN before. Our study on this novel RPUASN paradigm has been published in the December 2012 issue of the IEEE Sensors Journal [5].

In RPUASN, battery-free sensors are powered by a remote external acoustic source. In the proposed architecture, a typical RPUASN node consists four fundamental units. The *control, sensing and processing (CSP)* unit performs sensing and data processing. The exchange of information among RPUASN nodes is achieved through the *communication unit*, which contains an acoustic transducer. The acoustic transmission from the external power source

induces voltage on the *harvesting unit*, which consists of an array of hydrophones. These harvesting hydrophones operate at the transmission frequency of the external acoustic source, and they do not participate in communication. The power harvested at an RPUASN node can be used for operation or it can be stored in the *power unit*, which is made up of a rectifier and a reservoir capacitor.

The voltage generated in the harvesting unit depends on several parameters, such as the frequency and the power of the source, number and receiving sensitivity of harvesting hydrophones in the RPUASN node, and the attenuation in the underwater channel. In Chapter 2, the power harvested at an RPUASN node is analyzed and formulated according to the level of the induced voltage and characteristics of circuit components. It is shown by numerical examples that RPUASN operation with indefinite lifetime is practically realizable with appropriate selection of parameters.

In order to guarantee sensing coverage and communication connectivity in RPUASN, power harvesting characteristics of the nodes must be taken into account. 1-coverage implies that every location in the network is monitored by at least one node, which guarantees the communication connectivity of nodes at the same time. In order to cover a three dimensional region while maintaining connectivity for a random node deployment, it is vital to estimate the appropriate sensing range, transmission range, and node density. In Chapter 2, the minimum sensing range of an RPUASN node, the maximum volume of the network to be covered, and the number of nodes to achieve 1-coverage in the network are investigated for varying power requirements at nodes and for different deployment strategies. The deployment volume depends on the location and the directivity of the source. The source can be placed at the water surface, powering a spherical cone underwater, which is a realistic deployment scenario. Alternatively, the source can power a spherical volume around itself, if it is submerged in deep water.

6.1.2   X-PACCA Protocol

We identified SPUASN as a special case of RPUASN, where the data sink acts as the external acoustic power source of the network. In order to provide SPUASN with MAC, routing, and transport layer functionalities, we proposed X-PACCA, which is a cross-layer protocol based merely on the harvested power levels of SPUASN nodes. Route construction is performed with respect to differences of power levels harvested at nodes. Next hop selection and medium access priorities are given to nodes closer to the sink, resulting in a loop-free path to reduce end-to-end packet delay. MAC layer operates according to CSMA/CA rules at relay nodes. The initial backoff window size at a relay node is adapted according to the power differential between the previous sender and the relay node. Finally, transport layer reliability is achieved through packet acknowledgment by the data sink.

In X-PACCA, duplicate packet transmission is effectively suppressed, since nodes drop packets immediately when they hear the successful transmission of the same packet from a more powerful neighbor, i.e. one that is closer to the sink. Sink acknowledgments avoid repeated forwarding of event data. Moreover, X-PACCA does not need any network information or clock synchronization.

The effects of protocol parameters on end-to-end packet delivery performance are investigated through simulations. MAC and routing performances of X-PACCA are compared against several highly-cited protocols proposed for UASN. The cross-layer operation of X-PACCA

is also simulated for various node densities and data generation rates. The results of the performance evaluation show that appropriate selection of X-PACCA parameters satisfy latency reduction, collision avoidance, acceptable receive throughput and successful packet delivery objectives in SPUASN.

Investigation of cross-channel performance shows that utilizing a minimal number of nodes, sufficient to achieve 1-coverage, that is, minimal investment in terms of network cost, results in better end-to-end delay as well as packet delivery performance than deploying a higher number of sensors. This is clearly further justification of the feasibility of the RPUASN paradigm as well as the proposed X-PACCA protocol. Our X-PACCA protocol and related performance evaluations are also presented in our paper which is going to appear in the proceedings of MED-HOC-NET 2013 [6].

6.1.3   Channel Capacity and Characteristics in RPUASN

The RPUASN paradigm is studied in terms of the channel capacity, SINR, and BER achieved using different digital modulation types under various realistic conditions. In the analysis, it is assumed that the external acoustic power source is placed on the water surface, leading to a conical volume of sensor deployment. The capacity of the channel depends on the communication frequency, as well as the interference level among nodes. Instead of exploiting MAC protocols that ensure interference-free operation, upper and lower bounds of communication capacity are analyzed through silencing a portion of neighbors at each node. In addition to the SINR and BER characteristics, the differences between harvested power levels, and hence the sensing ranges of nodes also effect the theoretical limits of channel capacity in RPUASN. The results of the analysis reveal that a certain number of nodes should be kept silent for higher SINR and lower BER, providing better channel quality. Thus, the analysis on channel capacity provides the motivation for proposing the necessary MAC protocol constraints for RPUASN, in which feasible communication capacities can be reached with practical configurations and commercially available node components.

6.1.4   Literature Survey on MAC, Routing, and Transport Layer Protocols for UASN

Existing literature on MAC, routing, and transport layer protocols for UASN is reviewed, proposed solutions are briefly explained, classified, and compared according to their solution approaches. The objectives of the survey are: (1) to classify protocols and to determine their pros and cons, (2) to shape the characteristics of our new cross-layer X-PACCA protocol, and (3) to select the protocols to compare against X-PACCA in our performance evaluation. To the best of our knowledge, no survey covering the MAC, routing, and transport layer solutions has been presented in the literature.

According to their medium access strategies, MAC solutions proposed for UASN can be classified as deterministic, contention-based, CSMA-based, reservation-based, or ALOHA-based protocols. In most of the reservation-based solutions, nodes estimate network parameters such as propagation delays for scheduling transmissions; yet, this estimation is more applicable for static and slowly changing network conditions. CSMA and its variations have been preferred to avoid collisions in case of simultaneous transmission attempts, which occur frequently in ALOHA-based protocols. However, the handshaking-based approach in contention-based

and CSMA-based protocols requires synchronization of all nodes, which is impractical in the underwater environment with long propagation delay.

Most of the routing protocols operate on demand when it is required to relay collected data from underwater sensors to the data sink, and forwarding decisions are made at each hop. The operation of these protocols require either geographical or network state information. There are also some solutions that are based on routing table maintenance at nodes or end-to-end route decisions made at data sources. These solutions suffer from the spatio-temporal uncertainties in the underwater channel.

Only a few solutions have been proposed for the transport layer in UASN. Those solutions discuss the applicability of error control techniques for the selection of links that optimize power attenuation and transmission delay. ARQ-based protocols suffer from long propagation delay, packet traffic, and high energy consumption due to retransmissions. To reduce packet overhead, implicit ACKs can be deployed, or FEC techniques can be used. However, such solutions need coding methods with extra information such as link quality, required number of transmissions, and inter-node distances. Hybrid protocols benefit from the advantages of both ARQ and FEC, and they achieve packet recovery at the receiver side via low-complexity linear coding. Finally, some recent transport layer protocols that are based on network coding and biologically-inspired approaches require investigation under varying deployments and mobility levels.

The main performance criterion in these protocols is energy efficiency, since conventional UASN nodes run on limited-capacity batteries. Focusing only on the characteristics of the channel and adjusting source/sink parameters accordingly, RPUASN solution removes the main constraint in protocol design for underwater communications.

6.2   Future Work

As seen in Fig. 2.3, if a low-power source goes beyond 1 km, P_{harv} begins to drop below 1 mW. Even then, low duty cycles and long power storage periods would enable continued sensing, processing, and communication. These points deserve further study. While batteries are the most widely used storage devices, supercapacitors, also known as Electrochemical Double Layer Capacitors (EDLCs) or ultracapacitors, can substitute them with the help of recent advances in electronics and storage technologies [97]. Power demand profiles in communication networks generally require power pulses that are satisfied by batteries only by compromising their lifetime. Hence, batteries impose constraints for UASN in terms of both limited capacity and short lifetime.

Supercapacitors can be charged within 1/60 of the charging time of a conventional battery. Their cycle life is approximately 10^5 times longer than batteries, doubling the service lifetimes provided by the battery technology. Moreover, they provide very high specific power levels around 10 kW/kg. Details and examples related to the advantages of supercapacitors can be found in cites such as [98], [99], and [100]. Using fast-charging supercapacitors with higher storage limits, RPUASN nodes may operate on a *harvest-store-and-use* basis. Hence, the instantaneous power (P_{req}) to be harvested from the external acoustic source becomes lower, enabling the use of low-power sources and enlarging the network volume powered by the source. Lowering the power of the external acoustic source and adjusting its frequency can be desired to avoid eavesdropping in especially covert operations.

Since RPUASN consist of a large number of sensor nodes, the cost of a single node is crucial in justifying the overall cost of the networks. As a result, diminishing the cost of an RPUASN node is still a challenging issue, given the expected storage capabilities, application-specific processing requirements, and transducer design expenditures.

In this thesis, we assumed that the transmission and sensing patterns of RPUASN sensors were omnidirectional. The effects of transmission and sensing directivity levels of sensors may also be considered as a future study.

Another issue that deserves further study is the operation of RPUASN with multiple external acoustic power sources. Using multiple sources raises the following points of discussion:

- The power sources can also be used as data sinks as in SPUASN. Using multiple sinks may result in better performance in terms of lower delay and higher delivery success.

- The number and locations of the sources should be selected according to the power requirements of nodes.

- When more than one sources are available, it may be possible to use lower power levels at the sources, or instead of continuous power dissemination, they may operate with an appropriate powering cycle.

- The number of nodes needed to satisfy 1-coverage in the network depends on the power supplied from the sources and the minimum power required at the battery-free nodes.

- An RPUASN node fed by multiple sources may run on an on-off schedule according to the operation of the sources.

Since the volume powered by the sources determine the size and geometry of the network, these points must be considered simultaneously. Since sensor network protocols must possess self-organizing capabilities, the constraints to be determined can be related to various RPUASN parameters, such as physical conditions of the channel, network density, topology, traffic congestion, or route discovery. Therefore, the main challenges in the protocol design for RPUASN are channel characteristics such as multipath, attenuation, existence of shadow zones with no connectivity, and ambient noise. With the conventional power limitations removed, other possible challenges in the design of protocols can be the effects of storage techniques and using duty cycles at nodes to reduce interference and overhearing, as discussed above.

RPUASN may also involve a certain level of mobility, with sensors that can be either attached to AUVs, or drifting in water. While mobility can be useful [4] to maximize sensor coverage with limited hardware, it raises difficulties for localization of nodes, placement of sources, and maintenance of connectivity. In some cases, it may be necessary to incorporate Doppler-shift estimation to account for errors due to node mobility or water currents. Protocol operation in X-PACCA is based purely on local decisions, and sensor mobility, provided that it is not at severely high levels, would not have a detrimental effect on performance, but the conditions for this need further study.

The parameters discussed in the design of X-PACCA protocol are backoff constant k, slot length, power ratio β, and initial source window size W_s. Performance evaluation results reveal that appropriate selection of these parameters ensure acceptable latency, throughput, and delivery performance. Moreover, these parameters are closely related with the range and power

requirements of SPUASN nodes, as well as the determination of the network volume and sink parameters. Therefore, further investigation and optimization of X-PACCA parameters can provide valuable insight into development of SPUASN applications.

Since the development of underwater communications is driven by application requirements, it is possible to enable more underwater applications through achieving lower cost in computing, processing, sensing, and communication with cheaper transducers. The effective analysis, integration and testing of novel ideas, such as RPUASN, is of top importance to gain an insight into how successful practice fits proposed theory. Hence, the development of new computational models and simulation tools like Aqua-Sim is necessary, as well as the use of testbed deployments to increase the accuracy and the robustness of system characterization.

The effects of acoustic signals and transmission frequencies can also be studied to prevent harm to aquatic life and underwater habitats.

The capacity of a particular underwater acoustic channel depends strongly on frequency and range. Therefore, fixed channel allocation schemes do not perform well in underwater communications, and the applicability of cognitive radio and dynamic spectrum access to underwater communications can be investigated.

REFERENCES

[1] I. F. Akyildiz, D. Pompili, and T. Melodia, "Underwater acoustic sensor networks: research challenges," *Ad Hoc Networks*, vol. 3, no. 3, pp. 257-279, May 2005.

[2] M. Chitre, S. Shahabudeen, and M. Stojanovic, "Underwater acoustic communications and networking: Recent advances and future challenges," *Marine Technology Society Journal*, vol. 42, no. 1, pp. 103-116, Spring 2008.

[3] P. Casari and M. Zorzi, "Protocol design issues in underwater acoustic networks," *Computer Communications*, vol. 34, no. 17, pp. 2013-2025, Nov. 2011.

[4] J. Heidemann, M. Stojanovic, and M. Zorzi, "Underwater sensor networks: applications, advances and challenges," *Philosophical Transactions of the Royal Society A: Mathematical, Physical and Engineering Sciences*, vol. 370, no. 1958, pp. 158-175, Jan. 2012.

[5] A. Bereketli and S. Bilgen, "Remotely Powered Underwater Acoustic Sensor Networks," *IEEE Sensors Journal*, vol. 12, no. 12, pp. 3467-3472, Dec. 2012.

[6] A. Bereketli, H. Türken, and S. Bilgen, "Cross Layer Power Adaptive CSMA/CA for Sink Powered Underwater Acoustic Sensor Networks," to appear in *Proc. 12th Annual Mediterranean Ad Hoc Networking Workshop (Med-Hoc-Net)*, Ajaccio, Corsica, France, June 2013.

[7] J. Partan, J. Kurose, and B. N. Levine, "A Survey of Practical Issues in Underwater Networks," *ACM SIGMOBILE Mobile Computing and Communications Review*, vol. 11, no. 4, pp. 23-33, Oct. 2007.

[8] S. Sudevalayam and P. Kulkarni, "Energy harvesting sensor nodes: Survey and implications," *IEEE Commun. Surveys Tutorials*, vol. 13, no. 3, pp. 443-461, Jul. 2011.

[9] A. D. Waite, "Sonar for Practising Engineers," *Wiley*, 2002.

[10] A. Tabesh and L. G. Frechette, "A low-power stand-alone adaptive circuit for harvesting energy from a piezoelectric micropower generator," *IEEE Trans. Ind. Electron.*, vol. 57, no. 3, pp. 840-849, Mar. 2010.

[11] C. H. Sherman and J. L. Butler, "Transducers and Arrays for Underwater Sound," *Springer-Verlag*, 2007.

[12] M. Stojanovic and J. Preisig, "Underwater acoustic communication channels: Propagation models and statistical characterization," *IEEE Commun. Mag.*, vol. 47, no. 1, pp. 84-89, Jan. 2009.

[13] International Transducers Corporation, Santa Barbara, CA, "ITC Underwater Transducers," [Online]. Available: `http://www.itc-transducers.com/` [Apr. 12, 2013].

[14] I. Vasilescu, K. Kotay, D. Rus, M. Dunbabin, and P. Corke, "Data collection, storage, retrieval with an underwater sensor network," in *Proc. ACM SenSys'05*, pp. 154-165, Nov. 2005.

[15] N. Aslam and W. Robertson, "Distributed coverage and connectivity in three dimensional wireless sensor networks," in *Proc. ACM IWCMC'10*, pp. 1141-1145, 2010.

[16] V. Ravelomanana, "Extremal properties of three-dimensional sensor networks with applications," *IEEE Trans. Mobile Comput.*, vol. 3, no. 3, pp. 246-257, Jul.-Aug. 2004.

[17] D. Pompili, T. Melodia, and I. F. Akyildiz, "Deployment analysis in underwater acoustic wireless sensor networks," in *Proc. ACM WUWNet'06*, pp. 48-55, 2006.

[18] L. Freitag, M. Grund, S. Singh, J. Partan, P. Koski, and K. Ball, "The WHOI micro-modem: An acoustic communications and navigation system for multiple platforms," in *Proc. OCEANS 2005*, pp. 1086-1092, Sep. 2005.

[19] J. Wills, W. Ye, and J. Heidemann, "Low-power acoustic modem for dense underwater sensor networks," in *Proc. ACM WUWNet'06*, pp. 79-85, 2006.

[20] LinkQuest Inc., San Diego, CA, "SoundLink Underwater Acoustic Modems," [Online]. Available: `http://www.link-quest.com/` [Apr. 12, 2013].

[21] S. M. N. Alam and Z. J. Haas, "Coverage and connectivity in three-dimensional networks," in *Proc. ACM MobiCom'06*, pp. 346-357, Sep. 2006.

[22] L. M. Brekhovskikh and Yu. P. Lysanov, "Fundamentals of Ocean Acoustics," *Springer*, 1982.

[23] R. F. W. Coates, "Underwater Acoustic Systems," *Macmillan*, 1990.

[24] A. Stefanov and M. Stojanovic, "Design and performance analysis of underwater acoustic networks," *IEEE Journal on Selected Areas in Communications*, vol. 29, no. 10, pp. 2012-2021, Dec. 2011.

[25] R. Jurdak, C. V. Lopes, and P. Baldi, "Battery lifetime estimation and optimization for underwater sensor networks," *IEEE Sensor Network Operations*, pp. 397-420, 2004.

[26] M. Stojanovic, "On the relationship between capacity and distance in an underwater acoustic channel," *ACM SIGMOBILE Mobile Comp. Commun. Rev.*, vol. 11, no. 4, pp. 34-43, Oct. 2007.

[27] A. Goldsmith, "Wireless Communications," *Cambridge University Press*, 2005.

[28] C. Petrioli, R. Petroccia, and M. Stojanovic, "A comparative performance evaluation of MAC protocols for underwater sensor networks," in *Proc. OCEANS 2008*, pp. 1-10, Sep. 2008.

[29] X. Guo, M. R. Frater, and M. J. Ryan, "Design of a Propagation-Delay-Tolerant MAC Protocol for Underwater Acoustic Sensor Networks," *IEEE Journal of Oceanic Engineering*, vol. 34, no. 2, pp. 170-180, Apr. 2009.

[30] B. Peleato and M. Stojanovic, "Distance Aware Collision Avoidance Protocol for Ad-Hoc Underwater Acoustic Sensor Networks," *IEEE Communications Letters*, vol. 11, no. 12, pp. 1025-1027, Dec. 2007.

[31] Y. J. Chen and H. L. Wang, "Ordered CSMA: a collision-free MAC protocol for underwater acoustic networks," in *Proc. OCEANS 2007*, pp. 1-6, 2007.

[32] W.-H. Liao and C.-C. Huang, "SF-MAC: A Spatially Fair MAC Protocol for Underwater Acoustic Sensor Networks," *IEEE Sensors Journal*, vol. 12, no. 6, pp. 1686-1694, June 2012.

[33] M. Molins and M. Stojanovic, "Slotted FAMA: a MAC protocol for underwater acoustic networks," in *Proc. OCEANS 2006 - Asia Pacific*, pp. 1-7, May 2006.

[34] P. Xie and J.-H. Cui, "R-MAC: An Energy-Efficient MAC Protocol for Underwater Sensor Networks," in *Proc. WASA 2007*, pp. 187-198, Aug. 2007.

[35] A. A. Syed, W. Ye, and J. Heidemann, "T-Lohi: A New Class of MAC Protocols for Underwater Acoustic Sensor Networks," in *Proc. IEEE INFOCOM 2008*, pp. 231-235, Apr. 2008.

[36] M. K. Park and V. Rodoplu, "UWAN-MAC: An Energy-Efficient MAC Protocol for Underwater Acoustic Wireless Sensor Networks," *IEEE Journal of Oceanic Engineering*, vol. 32, no. 3, pp. 710-720, July 2007.

[37] N. Chirdchoo, W.-S. Soh, and K. C. Chua, "RIPT: A Receiver-initiated Reservation-based Protocol for Underwater Acoustic Networks," *IEEE Journal on Selected Areas in Communications*, vol. 26, no. 9, pp. 1744-1753, Dec. 2008.

[38] X. Guo, M. R. Frater, and M. J. Ryan, "A Propagation-delay-tolerant Collision Avoidance Protocol for Underwater Acoustic Sensor Networks," in *Proc. OCEANS 2006 - Asia Pacific*, pp. 1-6, May 2006.

[39] N. Chirdchoo, W.-S. Soh, and K. C. Chua, "Aloha-Based MAC Protocols with Collision Avoidance for Underwater Acoustic Networks," in *Proc. IEEE INFOCOM 2007*, pp. 2271-2275, May 2007.

[40] N. Chirdchoo, W.-S. Soh, and K. C. Chua, "MACA-MN: A MACA-based MAC Protocol for Underwater Acoustic Networks with Packet Train for Multiple Neighbors," in *Proc. IEEE VTC 2008*, pp. 46-50, May 2008.

[41] H.-H. Ng, W.-S. Soh, and M. Motani, "MACA-U: A Media Access Protocol for Underwater Acoustic Networks," in *Proc. IEEE GLOBECOM 2008*, pp. 1-5, 2008.

[42] D. Pompili, T. Melodia, and I. F. Akyildiz, "A CDMA-based Medium Access Control for UnderWater Acoustic Sensor Networks," *IEEE Transactions on Wireless Communications*, vol. 8, no. 4, pp. 1899-1909, Apr. 2009.

[43] C.-C. Hsu, K.-F. Lai, C.-F. Chou, and K. C.-J. Lin, "ST-MAC: Spatial-Temporal MAC Scheduling for Underwater Sensor Networks," in *Proc. IEEE INFOCOM 2009*, pp. 1827-1835, Apr. 2009.

[44] H.-H. Ng, W.-S. Soh, and M. Motani, "BiC-MAC: Bidirectional-Concurrent MAC protocol with packet bursting for underwater acoustic networks," in *Proc. IEEE OCEANS 2010*, pp. 1-7, Sep. 2010.

[45] M. K. Watfa, S. Selman, and H. Denkilkian, "UW-MAC: An underwater sensor network MAC protocol," *Int. J. Commun. Syst.*, vol. 23, no. 4, pp. 485-506, Apr. 2010.

[46] Y. Noh, P. Wang, U. Lee, D. Torres, and M. Gerla, "DOTS: A propagation Delay-aware Opportunistic MAC protocol for underwater sensor networks," in *Proc. 18th IEEE International Conference on Network Protocols (ICNP)*, pp. 183-192, Oct. 2010.

[47] J. Ni, B. Tan, and R. Srikant, "Q-CSMA: Queue-Length-Based CSMA/CA Algorithms for Achieving Maximum Throughput and Low Delay in Wireless Networks," *IEEE/ACM Transactions on Networking*, vol. 20, no. 3, pp. 825-836, June 2012.

[48] H.-H. Ng, W.-S. Soh, and M. Motani, "ROPA: A MAC Protocol for Underwater Acoustic Networks with Reverse Opportunistic Packet Appending," in *Proc. IEEE WCNC 2010*, pp. 1-6, Apr. 2010.

[49] W. Lin, E. Cheng, and F. Yuan, "EHM: a novel efficient protocol based handshaking mechanism for underwater acoustic sensor networks," *Wireless Networks*, pp. 1-11, Oct. 2012.

[50] Y. Luo, L. Pu, Z. Peng, Z. Zhou, and J.-H. Cui, "CT-MAC: a MAC protocol for underwater MIMO based network uplink communications," in *Proc. Seventh ACM International Conference on Underwater Networks and Systems (WUWNet '12)*, Nov. 2012.

[51] K. Kredo, P. Djukic, and P. Mohapatra, "STUMP: Exploiting Position Diversity in the Staggered TDMA Underwater MAC Protocol," in *Proc. IEEE INFOCOM 2009*, pp. 2961-2965, Apr. 2009.

[52] J. Ma and W. Lou, "Interference-aware spatio-temporal link scheduling for long delay underwater sensor networks," in *Proc. IEEE SECON 2011*, pp. 431-439, June 2011.

[53] M. Ayaz, I. Baig, A. Abdullah, and I. Faye, "A survey on routing techniques in underwater wireless sensor networks," *Journal of Network and Computer Applications (Elsevier)*, vol. 34, no. 6, pp. 1908-1927, Nov. 2011.

[54] J.-P. Jornet, M. Stojanovic, and M. Zorzi, "Focused beam routing protocol for underwater acoustic networks," in *Proc. the third ACM international workshop on Underwater Networks (WuWNeT)*, pp. 75-82, Sep. 2008.

[55] J. Chen, X. Wu, and G. Chen, "REBAR: A Reliable and Energy Balanced Routing Algorithm for UWSNs," in *Proc. Seventh International Conf. on Grid and Cooperative Computing (GCC)*, pp. 349-355, Oct. 2008.

[56] P. Xie, J.-H. Cui, and L. Lao, "VBF: Vector-Based Forwarding Protocol for Underwater Sensor Networks," in *Proc. Networking 2006*, vol. 3976, pp. 3467-3472, May 2006.

[57] H. Yan, J. Shi, and J.-H. Cui, "DBR: Depth-Based Routing for Underwater Sensor Networks," in *Proc. Networking 2008*, vol. 4982, pp. 72-86, May 2008.

[58] M. Hill, P. Wang, Y. Noh, L. Vieira, M. Gerla, and J.-H. Cui, "Pressure Routing for Underwater Sensor Networks," in *Proc. IEEE INFOCOM 2010*, pp. 1-9, Mar. 2010.

[59] D. Shin, D. Hwang, and D. Kim, "DFR: an efficient directional flooding-based routing protocol in underwater sensor networks," *Wirel. Commun. Mob. Comput.*, vol. 12, no. 17, pp. 1517-1527, Dec. 2012.

[60] Y. Noh, U. Lee, P. Wang, B. S. C. Choi, and M. Gerla, "VAPR: Void Aware Pressure Routing for Underwater Sensor Networks," *IEEE Transactions on Mobile Computing*, vol. 12, no. 5, pp. 895-908, May 2013.

[61] S. Gopi, K. Govindan, D. Chander, U. B. Desai, and S. N. Merchant, "PULRP: Path Unaware Layered Routing Protocol for Underwater Sensor Networks," in *Proc. IEEE ICC 2008*, pp. 3141-3145, May 2008.

[62] T. Hu and Y. Fei, "QELAR: A Machine-learning-based Adaptive Routing Protocol for Energy-efficient and Lifetime-extended Underwater Sensor Networks," *IEEE Transactions on Mobile Computing*, vol. 9, no. 6, pp. 796-809, June 2010.

[63] S. T. Nguyen, E. Cayirci, L. Yan, and C. Rong, "A Shadow Zone Aware Routing Protocol for Acoustic Underwater Sensor Networks," *IEEE Communications Letters*, vol. 13, no. 5, pp. 366-368, May 2009.

[64] S. Gopi, K. Govindan, D. Chander, U. B. Desai, and S. N. Merchant, "E-PULRP: Energy Optimized Path Unaware Layered Routing Protocol for Underwater Sensor Networks," *IEEE Transactions on Wireless Communications*, vol. 9, no. 11, pp. 3391-3401, Nov. 2010.

[65] D. Pompili and T. Melodia, "Three Dimensional Routing in Underwater Acoustic Sensor Networks," in *Proc. ACM PE-WASUN'05*, pp. 214-221, Oct. 2005.

[66] M. C. Domingo, "A Distributed Energy-Aware Routing Protocol for Underwater Wireless Sensor Networks," *Wireless Personal Communications*, vol. 57, no. 4, pp. 607-627, Apr. 2011.

[67] M. Al-Bzoor, Y. Zhu, J. Liu, A. Reda, J.-H. Cui, and S. Rajasekaran, "Adaptive Power Controlled Routing for Underwater Sensor Networks," *Wireless Algorithms, Systems, and Applications (Springer)*, vol. 7405, pp. 549-560, 2012.

[68] S. Basagni, C. Petrioli, R. Petroccia, and D. Spaccini, "Channel-aware Routing for Underwater Wireless Networks," in *Proc. OCEANS 2012*, pp. 1-9, May 2012.

[69] Y.-S. Chen and Y.-W. Lin, "Mobicast Routing Protocol for Underwater Sensor Networks," *IEEE Sensors Journal*, vol. 13, no. 2, pp. 737-749, Feb. 2013.

[70] J. W. Lee, J. Y. Cheon, and H.-S. Cho, "A cooperative ARQ scheme in underwater acoustic sensor networks," in *Proc. OCEANS 2010*, pp. 1-5, May 2010.

[71] Z. Zhou, H. Mo, Y. Zhu, Z. Peng, J. Huang, and J.-H. Cui, "Fountain code based Adaptive multi-hop Reliable data transfer for underwater acoustic networks," in *Proc. IEEE ICC 2012*, pp. 6396-6400, June 2012.

[72] H. Tan, W. K. G. Seah, and L. Doyle, "A Multi-hop ARQ Protocol for Underwater Acoustic Networks," in *Proc. OCEANS 2007*, pp. 1-6, June 2007.

[73] J.-W. Lee, J.-P. Kim, J.-H. Lee, Y. S. Jang, K. C. Dho, K. Son, and H.-S. Cho, "An Improved ARQ Scheme in Underwater Acoustic Sensor Networks," in *Proc. OCEANS 2008*, pp. 1-5, Apr. 2008.

[74] S. Cai, Z. Gao, D. Yang, and N. Yao, "A network coding based protocol for reliable data transfer in underwater acoustic sensor," *Ad Hoc Networks*, [Online]. Available: `http://dx.doi.org/10.1016/j.adhoc.2013.02.001` [Feb. 27, 2013].

[75] S. Cai, Z. Gao, D. Yang, J. Zhao, and Y. Zhao, "IPool-ADELIN: An extended ADELIN based on IPool node for reliable transport of Underwater Acoustic Sensor Networks," *Ad Hoc Networks*, [Online]. Available: `http://dx.doi.org/10.1016/j.adhoc.2011.01.012` [Apr. 28, 2011].

[76] B. Liu, F. Garcin, F. Ren, and C. Lin, "A Study of Forward Error Correction Schemes for Reliable Transport in Underwater Sensor Networks," in *Proc. IEEE SECON'08*, pp. 197-205, June 2008.

[77] D. Shin and D. Kim, "FRT: Fast and reliable transport protocol for underwater wireless sensor networks," in *Proc. IEEE APSCC 2009*, pp. 402-407, Dec. 2009.

[78] B. Liu, H. Chen, X. Lei, F. Ren, and K. Sezaki, "Internode distance-based redundancy reliable transport in underwater sensor networks," *EURASIP Journal on Wireless Communications and Networking*, vol. 2010, pp. 1-16, Apr. 2010.

[79] R. Cao and L. Yang, "Reliable transport and storage protocol with fountain codes for underwater acoustic sensor networks," in *Proc. ACM WUWNet'10*, pp. 18-21, 2010.

[80] J. Xu, K. Li, and G. Min, "Reliable and Energy-Efficient Multipath Communications in Underwater Sensor Networks," *IEEE Transactions on Parallel and Distributed Systems*, vol. 23, no. 7, pp. 1326-1335, July 2012.

[81] D. Shin, S. Lee, and D. Kim, "Location-based k-ACK aggregation method for underwater sensor networks," in *Proc. OCEANS 2011*, pp. 1-5, Sep. 2011.

[82] H. Mo, A. C. Mingir, H. Alhumyani, Y. Albayram, and J.-H. Cui, "UW-HARQ: An underwater hybrid ARQ scheme: Design, implementation and initial test," in *Proc. OCEANS 2012*, pp. 1-5, Oct. 2012.

[83] P. Xie, Z. Zhou, Z. Peng, J.-H. Cui, and Z. Shi, "SDRT: A reliable data transport protocol for underwater sensor networks," *Ad Hoc Networks*, vol. 8, no. 7, pp. 708-722, Sep. 2010.

[84] G. Lv, Z. Guo, H. Qu, and Z. Che, "Study of RFEC-Based Transport Protocol in Underwater Acoustic Sensor Networks," in *Proc. WiCOM'08*, pp. 1-4, Oct. 2008.

[85] Z. Guo, B. Wang, P. Xie, W. Zeng, and J.-H. Cui, "Efficient error recovery with network coding in underwater sensor networks," *Ad Hoc Networks*, vol. 7, no. 4, pp. 791-802, June 2009.

[86] M. C. Domingo, "Marine communities based congestion control in underwater wireless sensor networks," *Information Sciences*, vol. 228, pp. 203-221, Apr. 2013.

[87] P. Xie *et al.*, "Aqua-Sim: An NS-2 based simulator for underwater sensor networks," in *Proc. OCEANS 2009, MTS/IEEE Biloxi - Marine Technology for Our Future: Global and Local Challenges*, pp. 1-7, Oct. 2009.

[88] The VINT Project. "The ns Manual." [Online]. Available: `http://www.isi.edu/nsnam/ns/`, 2002 [Mar. 14, 2013].

[89] M. Tran *et al.*, "Aqua-3D: An underwater network animator," in *Proc. OCEANS 2012*, pp. 1-5, Oct. 2012.

[90] Aqua-Sim - obinet. "Aqua-Sim Overview." [Online]. Available: `http://obinet.engr.uconn.edu/wiki/index.php/Aqua-Sim`, 2009-2013 [Apr. 24, 2013].

[91] METUTECH Technology Transfer Office (TTO) and Yalçıner Patent ve Danışmanlık Ltd. Şti., "Uzaktan Enerji Beslemeli Sualtı Akustik Algılayıcı Ağları," *Confidential Report*, Feb. 27, 2013.

[92] European Patent Office. "Espacenet Patent Search." [Online]. Available: `http://worldwide.espacenet.com/`, [Apr. 26, 2013].

[93] WIPO Patent Information Products and Services. "Patentscope." [Online]. Available: `http://patentscope.wipo.int/search/en/structuredSearch.jsf`, [Apr. 26, 2013].

[94] Türk Patent Enstitüsü. "Patent/Faydalı Model Araştırma." [Online]. Available: `http://online.tpe.gov.tr/EPATENT/servlet/PreSearchRequestManager`, [Apr. 26, 2013].

[95] Elsevier. "ScienceDirect Scientific Database." [Online]. Available: `http://www.sciencedirect.com/`, [Apr. 26, 2013].

[96] RSC Publishing. "RSC Advances." [Online]. Available: `http://pubs.rsc.org/en/journals/journalissues/ra#!recentarticles&all`, [Apr. 26, 2013].

[97] T. C. Kazmierski, G. V. Merrett, L. Wang, B. M. Al-Hashimi, A. S. Weddell, and I. N. Ayala-Garcia, "Modeling of Wireless Sensor Nodes Powered by Tunable Energy Harvesters: HDL-Based Approach," *IEEE Sensors Journal*, vol. 12, no. 8, pp. 2680-2689, Aug. 2012.

[98] Maxwell Technologies. "An Overview of Ultracapacitor Technology." [Online]. Available: `http://www.maxwell.com/ultracapacitors/`, [Apr. 29, 2013].

[99] Digi-Key Corporation. "Electric Double Layer Capacitors, Supercaps." [Online]. Available: `http://www.digikey.com/product-search/en/capacitors/electric-double-layer-capacitors-supercaps/131084`, [Apr. 29, 2013].

[100] Tecate Group. "Cap-XX Supercapacitors." [Online]. Available: `http://www.tecategroup.com/ultracapacitors-supercapacitors/cap-xx.php`, [Apr. 29, 2013].

CURRICULUM VITAE

PERSONAL INFORMATION

Surname, Name: Bereketli, Alper
Nationality: Turkish (TC)
Date and Place of Birth: 04.08.1980, İzmir
Marital Status: Married
Email: alperbereketli@gmail.com
Web: `http://www.eee.metu.edu.tr/~balper`

EDUCATION

Degree	Institution	Year of Graduation
M.S.	Electrical and Electronics Engineering, METU	2005
B.S.	Electrical and Electronics Engineering, METU	2002
High School	Karşıyaka Anadolu Lisesi, İzmir	1998

PROFESSIONAL EXPERIENCE

Year	Place	Enrollment
2009-Present	METEKSAN Savunma Sanayii A.Ş.	Chief Systems Engineer
2002-2009	Electrical and Electronics Engineering, METU	Research and Teaching Assistant
2001 July	ASELSAN A.Ş.	Intern Engineer
2000 July	ASELSAN A.Ş.	Intern Engineer

FOREIGN LANGUAGES

English (Fluent)
German (Intermediate)

PUBLICATIONS

- Alper Bereketli, Hasan Türken, and Semih Bilgen, ''Cross Layer Power Adaptive CSMA/CA for Sink Powered Underwater Acoustic Sensor Networks,'' to appear in *Proc. 12th Annual Mediterranean Ad Hoc Networking Workshop (Med-Hoc-Net)*, Ajaccio, Corsica, France, June 2013.

- Alper Bereketli and Semih Bilgen, ''Remotely Powered Underwater Acoustic Sensor Networks,'' *IEEE Sensors Journal*, vol. 12, no. 12, pp. 3467-3472, Dec. 2012.

- Alper Bereketli and Özgür B. Akan, "Communication Coverage in Wireless Passive Sensor Networks," *IEEE Communications Letters*, vol. 13, no. 2, pp. 133-135, Feb. 2009.

- Alper Bereketli and Özgür B. Akan, "Event-to-Sink Directed Clustering in Wireless Sensor Networks," in *Proc. WCNC 2009*, Budapest, Hungary, April 2009.

- Alper Bereketli and Özgür B. Akan, "Tactical Wireless Sensor Networks: Applications and Challenges," in *NATO-ARW Volume*, Edited by S. Olariu, 2007.

- Barış Atakan, Alper Bereketli, and Özgür B. Akan, "Homeostasis-based Multimedia Transport in Wireless Sensor Networks," *WOrkshop on advances in Wireless NETworking (WOW-NET)*, IFIP Networking 2007, Atlanta, USA, May 2007.

- Tamer Güdü, Taner Kolçak, Alper Bereketli, Selçuk Koçyiğit, and Selçuk Alparslan, "A Scalable Hardware Architecture for High Performance Acoustic Beamforming," to appear in *Proc. Undersea Defence Technology (UDT)*, Hamburg, Germany, June 2013.